

Journal Pre-proof

Synthesis and discovery of new compounds bearing coumarin scaffold for the treatment of pulmonary fibrosis

Dexin Deng, Heying Pei, Tingxuan Lan, Jiali Zhu, Minghai Tang, Linlin Xue, Zhuang Yang, Shoujun Zheng, Haoyu Ye, Lijuan Chen



PII: S0223-5234(19)30942-0

DOI: <https://doi.org/10.1016/j.ejmech.2019.111790>

Reference: EJMECH 111790

To appear in: *European Journal of Medicinal Chemistry*

Received Date: 14 August 2019

Revised Date: 7 October 2019

Accepted Date: 14 October 2019

Please cite this article as: D. Deng, H. Pei, T. Lan, J. Zhu, M. Tang, L. Xue, Z. Yang, S. Zheng, H. Ye, L. Chen, Synthesis and discovery of new compounds bearing coumarin scaffold for the treatment of pulmonary fibrosis, *European Journal of Medicinal Chemistry* (2019), doi: <https://doi.org/10.1016/j.ejmech.2019.111790>.

This is a PDF file of an article that has undergone enhancements after acceptance, such as the addition of a cover page and metadata, and formatting for readability, but it is not yet the definitive version of record. This version will undergo additional copyediting, typesetting and review before it is published in its final form, but we are providing this version to give early visibility of the article. Please note that, during the production process, errors may be discovered which could affect the content, and all legal disclaimers that apply to the journal pertain.

© 2019 Published by Elsevier Masson SAS.

Synthesis and discovery of new compounds bearing coumarin scaffold for the treatment of pulmonary fibrosis

Dexin Deng ^{a, 1}, Heying Pei ^{a, 1}, Tingxuan Lan ^a, Jiali Zhu ^a, Minghai Tang ^a, Linlin Xue ^a, Zhuang Yang ^a, Shoujun Zheng ^a, Haoyu Ye ^a, Lijuan Chen ^{a, *}

a. State Key Laboratory of Biotherapy and Cancer Center, West China Hospital, Sichuan University and Collaborative Innovation Center, Chengdu, 610041, China

* Corresponding authors. Lab of Natural Product Drugs, State Key Laboratory of Biotherapy and Cancer Center, West China Medical School, West China Hospital, Sichuan University, Chengdu 610041, PR China.

¹ Both authors contributed equally to this study.

Abstract:

Idiopathic pulmonary fibrosis, characterized by excess accumulation of extracellular matrix, involved in many chronic diseases or injuries, threatens human health greatly. We have reported a series of compounds bearing coumarin scaffold which potently inhibited TGF- β -induced total collagen accumulation in NRK-49F cell line and migration of macrophages. Compound **9d** also suppressed the TGF- β -induced protein expression of COL1A1, α -SMA, and p-Smad3 in vitro. Meanwhile, **9d** at a dose of 100 mg/kg/day through oral administrations for 4 weeks effectively alleviated infiltration of inflammatory cells in lung tissue and fibrotic

degree in bleomycin-induced pulmonary fibrosis model, which may related to its inhibition of TGF- β /Smad3 pathway and anti-inflammation efficacy. In addition, **9d** demonstrated decent bioavailability ($F = 39.88\%$) and suitable eliminated half-life time ($T_{1/2} = 13.09$ h), suggesting that **9d** could be a potential drug candidate for the treatment of fibrotic diseases.

Keywords:

Coumarins; Collagen accumulation; Anti-fibrosis; Anti-inflammatory; Pulmonary fibrosis.

1. Introduction

Idiopathic pulmonary fibrosis (**IPF**), characterized by exaggerated angiogenesis, fibro proliferation, and deposition of extracellular matrix, is a fatal type of fibrotic disease occurred in lung [1, 2]. Progressive scarring or fibrosis is confined to the interstitium of the lungs, leading to loss of lung function and eventual death [3-6]. Inflammation, due to the systemic and local responses of living tissues towards injury, also plays an important role in the development of fibrosis. Tissue damage recruits a variety of immunocytes and activates a series of pathologic responses, leading from tissue damage to inflammation, inflammation to fibrosis and fibrosis to function dysfunction [7, 8]. Meanwhile, migration of macrophages (a kind of inflammatory cell) driven by fibroblasts has shown to play a key part in evoking inflammatory

responses during tissue injury, leading to further fibrillation [9-11]. In a word, fibrosis is aggravated by the feedback loop between fibroblasts activation and inflammation.

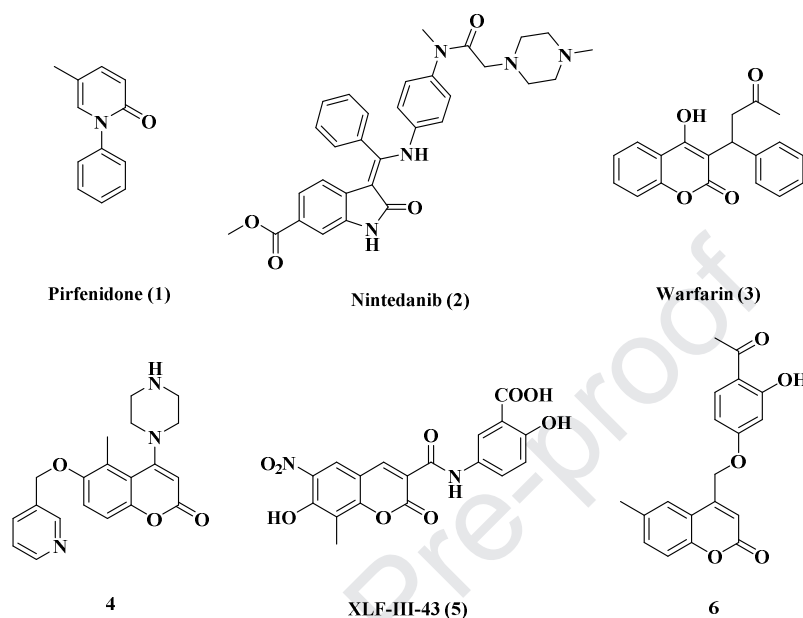


Figure 1. Structure of **Pirfenidone**, **Nintedanib** and other compounds bearing coumarin scaffold

At present, there are very few small molecule compounds approved for the treatment of fibrotic diseases. So far, only **Pirfenidone (1)** and **Nintedanib (2)** have been approved by FDA to treat for **IPF**. The major antifibrotic mechanism of **Pirfenidone** is considered to inhibit the TGF- β pathway, and proinflammatory cytokines such as TNF- α , IL-6, and IFN- γ have also been found to be inhibited [12]. **Nintedanib**, known as a small-molecule kinase inhibitor, mainly targets three receptor classes (VGFR, PDGFR, FGFR) involved in blood vessel formation and angiogenesis [13-15]. However, oral bioavailability of **Nintedanib** is approximately 12% in rats and 13% to 24% in monkeys [16]. Additionally, some side effects have been reported during the medication, such as diarrhea, nausea, and abdominal pain

[16]. Hence, low bioavailability and adverse side effects derived by multiple targets actually limit **Nintedanib** in further clinical treatment.

Coumarins, widely found in nature, known as a family of nature-occurring lactones first isolated from Tonka beans in 1820. Over 1300 coumarins have been identified, being reported to have multiple biological activities [17] treating diverse ailments. **Warfarin (3)**, a coumarins' derivative, known as a traditional anticoagulant, has been tested its treatment in idiopathic pulmonary fibrosis (Anticoagulant Effectiveness in Idiopathic Pulmonary Fibrosis, ACE-IPF) trial [18] for the prothrombotic state is 4 times higher in patients with IPF [19]. However, this program has been terminated because of increased deaths in the **Warfarin** group. Despite these unfavorable reports, using a new anticoagulant therapeutic strategy still is a hopefully strategy to improve patient's fibrotic states. Compound **4** (4-(1-piperazinyl) coumarins derivatives) also was proved to be a potent inhibitor of human platelet aggregation ($IC_{50}=37$ nM) in vitro [20]. **XLF-III-43 (5)**, a novel coumarin-aspirin compound, inhibits the expressions of CML-AGE, TGF- β 1, CTGF, fibronectin and collagen IV in kidneys [21]. Coumarin derivatives or analogues are also potential candidates for development of anti-inflammatory drugs [22]. Compound **6** possess obviously anti-inflammatory and analgesic activity in Carrageenin-induced paw edema in rats [23].

Encouraged by the anticoagulant, anti-platelet aggregation, anti-fibrosis and anti-inflammatory of coumarins, we designed a series of novel compounds using hybridizing coumarin skeleton (Figure 2) and hydrophobic group of **Nintedanib** to

improve the oral bioavailability and decrease the side effects. The anti-fibrosis and anti-inflammatory mechanism involved in fibrosis of the optimized compounds were also investigated both in vitro and in vivo.

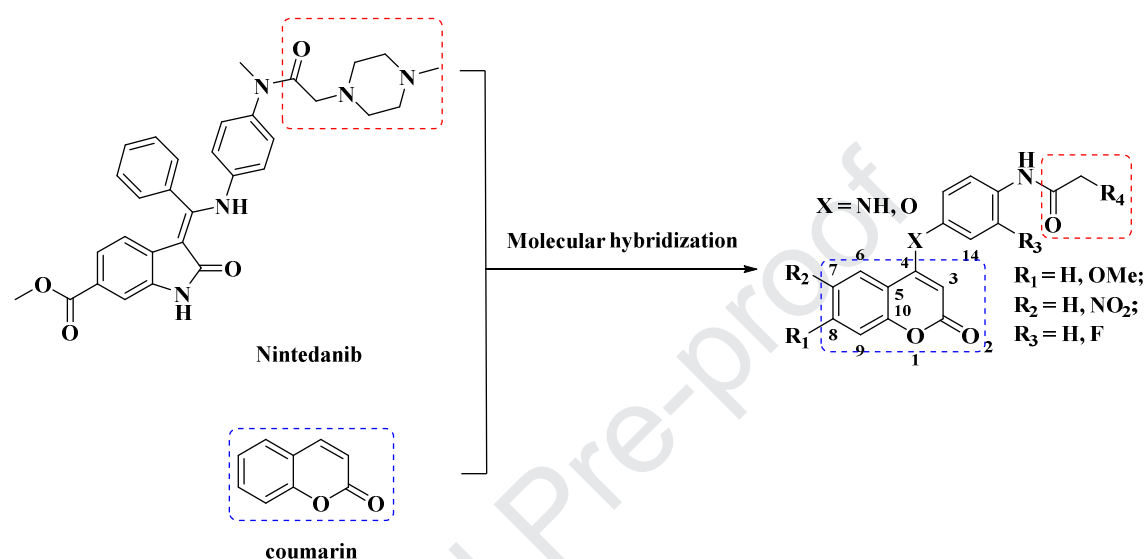


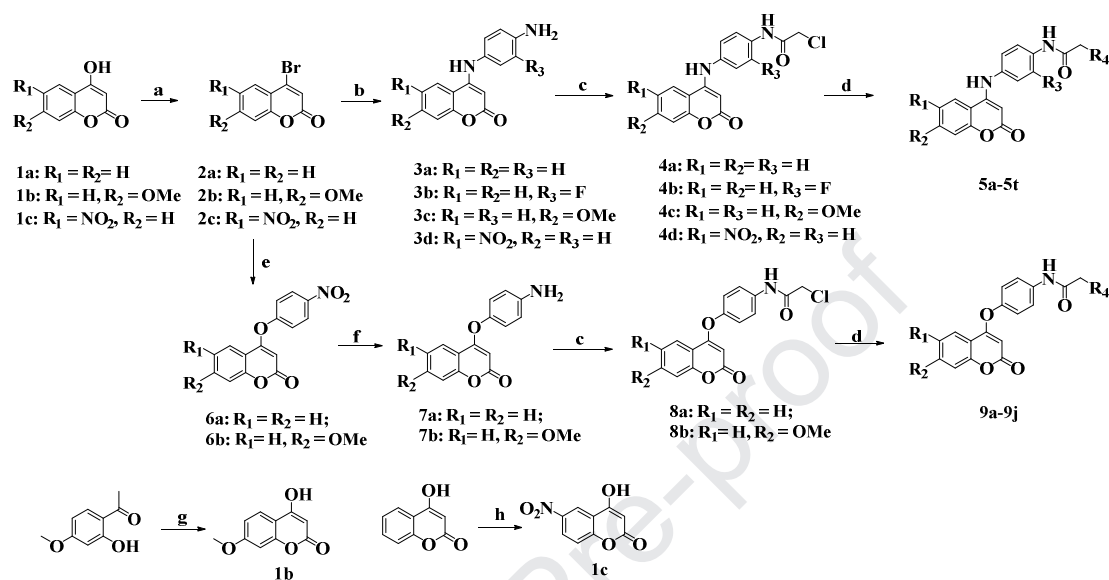
Figure 2. Design a novel series of compounds with anti-fibrotic effects by hybridizing coumarin skeleton and hydrophobic group of Nintedanib.

2. Results and discussion

2.1 Chemistry

At the beginning, we consider the effect of the different hydrophobic group to its anti-fibrotic biological activity. Compounds **5a-5e** were prepared by the synthesis method outlined in **Scheme 1**. 4-hydroxycoumarin (**1**) was reacted with TABA (Tetrabutylammonium bromide) and P_2O_5 in acetonitrile refluxing at 90 °C for 4 h, giving the important intermediate **2** that allowed completely reaction with benzene-1,4-diamine to offer **3** in a good yield. **3** was treated with chloroacetyl chloride in dry

DMF at 0-5°C to provide **4**, which was introduced with a variety of aliphatic amine via substitution reaction to give the final compounds **5a-5e**.



Scheme 1. Reagents and conditions: (a) TABA, P₂O₅, acetonitrile, 90 °C, 4 h. (b) Et₃N, EtOH, 70 °C, 2 h, rt, 4 h. (c) Chloroacetyl chloride, Et₃N, DMF, 0 °C, 3 h. (d) DMF, KI, rt, 3 h. (e) K₂CO₃, acetone, 65°C, overnight. (f) Pd/C, H₂, MeOH, rt, 3 h. (g) NaH, diethyl carbonate, 0 °C for 1h, then heated to 100 °C for further 3 h. (h) Sodium nitrate, concentrated sulphuric acid, 0 °C for 4h.

Then we initially researched the relationship between the position of the substituents in coumarins and its anti-fibrotic effects. Methoxy was added to the C-8 of coumarin to give **5k-5o**. 1-(2-hydroxy-4-methoxyphenyl)ethan-1-one) was reacted with diethyl carbonate and sodium hydride in diethyl carbonate at 0-5 °C for 1 h, then refluxed at 100 °C for 3 h to obtain Intermediate **2b**. The following processes were described as **5a-5e**, eventually giving target compounds **5k-5o**. To search the SAR of

electron-withdrawing substituent such as fluorine-containing and nitro group, other two kinds of analogues **5f-5j** and **5p-5t** were synthesized also according to Scheme 1, which was same as the procedures of **5a-5e**.

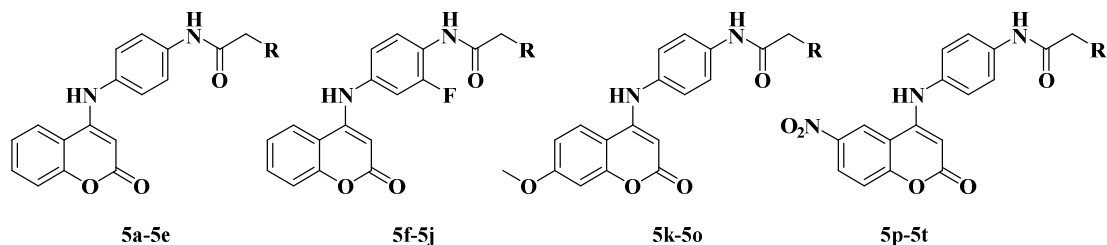
Finally, in consideration of bioisosteres, we'd like to explore the importance of linker N atom, which were subsequently substituted by O atom listed in **Scheme 1**. Intermediate **6a (6b)** was obtained by **2a (2b)** and 4-nitrophenol refluxed in acetone overnight. The following processes were described as **5a-5e**. Eventually, we got new series compounds **9a-9j**.

2.2. Biology

2.2.1 Inhibition of total collagen accumulation on NRK-49F cells

Excessive extracellular matrix (ECM), which is mainly composed of collagen, is a pathological marker of fibrotic disease, so detection of collagen synthesis is an effective indicator for evaluating fibrotic diseases. According to our previous research and other reports, rat fibroblast cells (NRK-49F) induced by TGF- β would produce much extracellular collagen that similar to the feature of fibrosis in vivo [24-26]. Thus, it has been recognized an effective and convenient method for anti-fibrotic screening model in vitro.

Compounds **5a-5t** were preliminarily screened for their effects on inhibiting total collagen accumulation induced by TGF- β in the NRK-49F cell line at a concentration of 10 μ M and the cell survival rate was calculated by MTT assay in NRK-49F cells for toxicity. Nintedanib was chosen as positive control.

Table 1 Collagen accumulation inhibition and cell survival rate of **5a-5t**.

Entry	R	Inhibition%	Survival%	Entry	R	Inhibition%	Survival%
		@ 10 μ M	@ 10 μ M			@ 10 μ M	@ 10 μ M
5a		26.82 \pm 4.84	87.54 \pm 3.25	5k		80.20 \pm 2.10	87.22 \pm 2.37
5b		41.83 \pm 3.22	75.24 \pm 1.21	5l		72.92 \pm 1.27	89.13 \pm 4.54
5c		80.21 \pm 2.30	91.48 \pm 1.52	5m		72.71 \pm 2.30	90.11 \pm 2.31
5d		75.21 \pm 7.07	43.63 \pm 1.96	5n		74.47 \pm 1.63	41.33 \pm 1.48
5e		12.43 \pm 2.18	62.04 \pm 1.37	5o		15.72 \pm 3.46	52.05 \pm 2.17
5f		36.84 \pm 2.82	78.06 \pm 1.50	5p		22.26 \pm 1.39	32.06 \pm 3.17
5g		34.54 \pm 3.68	72.35 \pm 3.52	5q		31.67 \pm 2.34	23.11 \pm 2.65
5h		21.90 \pm 2.13	88.47 \pm 4.22	5r		28.73 \pm 1.40	17.82 \pm 1.44
5i		11.33 \pm 1.87	67.70 \pm 2.52	5s		15.37 \pm 0.84	20.34 \pm 2.60
5j		33.30 \pm 6.33	74.27 \pm 3.84	5t		17.90 \pm 1.53	45.32 \pm 2.38
				Nintedanib		95.47 \pm 2.65	40.02 \pm 2.46

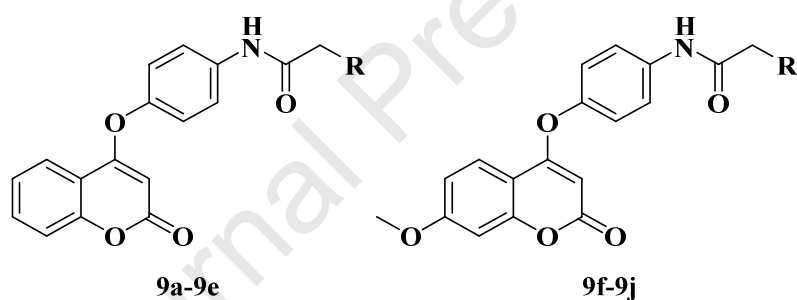
Inhibitory against TGF- β -induced total collagen accumulation in NRK-49F cells at a concentration of 10 μ M. Cell survival rate is calculated by MTT assay. The results are the means \pm SD of at least three independent experiments.

As shown in Table 1, compound **5c** possessed the good inhibition of collagen accumulation with weaker toxicity in NRK-49F cells among **5a-5e**. Meanwhile, methoxy introducing to the C-8 position of coumarin was taken into account to give compounds **5k-5o**. The collagen inhibition of these compounds generally superior to **5a-5b** and have little effect on toxicity, indicating that electron-donating ability of the substituents at C-8 may contribute to its bioactivity. Compounds **5d** and **5n** owned piperidyl terminal also have good inhibition, but they showed toxicity in vitro to some extent. As compounds bearing penta cyclic ring such as pyrrolidine (**5e** and **5o**) have little inhibitory activity. Compounds which have substitution of F atom on benzene ring were designed initially to improve biological activity. In fact, although the inhibitions of **5f-5j** were not improved, they have little effects on toxicity compared to **5a-5d**. However, compounds owned electron-hogging substituents at C-6 generally (**5p-5t**) have neither inhibition of collagen accumulation nor low toxicity.

Though **Nintedanib** showed excellent inhibition of collagen accumulation in NRK-49F cells, it was proved to inhibit collagen accumulation via killing cells, which is consistent with the observed phenomenon under the microscope (Figure 3). To reduce toxicity of compounds, bioisosteres, a principle and method widely used in

drug design, was then applied to subsequent compound designs to get compounds **9a-9e**. Specifically, the linker N atom was subsequently substituted by O atom and hopefully to reduce its toxicity. As we expected, all compounds in Table 2 have little effect on cell proliferation outstandingly compared to **5a-5t**. Methoxy group at C-8 position has no influence on cell proliferation, which means the linker atom O plays an important role in reducing the toxicity of compounds. Only compounds **9d** and **9g** show best biological activity among them.

Table 2 Collagen accumulation inhibition and cell survival rate of **9a-9j**



Entry	R	Inhibition% @ 10 μ M	Survival% @ 10 μ M	Entry	R	Inhibition% @ 10 μ M	Survival% @ 10 μ M
9a		24.04 \pm 1.63	83.57 \pm 3.26	9f		65.36 \pm 2.66	95.61 \pm 5.37
9b		34.63 \pm 2.37	97.05 \pm 3.18	9g		78.33 \pm 2.17	96.54 \pm 2.58
9c		75.32 \pm 3.24	98.02 \pm 2.43	9h		32.60 \pm 2.64	90.47 \pm 8.99
9d		85.14 \pm 1.32	93.62 \pm 1.94	9i		73.46 \pm 2.54	90.43 \pm 2.51
9e		18.80 \pm 3.48	82.94 \pm 2.36	9j		8.07 \pm 1.25	93.34 \pm 3.29
				Nintedanib		95.47 \pm 2.65	40.02 \pm 2.46

Inhibitory against TGF- β -induced total collagen accumulation in NRK-49F cells at a concentration of 10 μ M. Cell survival rate is calculated by MTT assay. The results are the means \pm SD of at least three independent experiments.

The terminal of hydrophobic group affects the inhibition activity to some extent. Compounds owned different structures which distinguished their biological activity even they have the same hydrophobic group at terminal. However, compounds owned pyrrolidine (**5e**, **5o**, **9e**, **9j**) both have little inhibitory activity to collagen accumulation. Modifications with electron-withdrawing group seemed unpopular. More important, substitution of the linker N atom with O atom was successfully to improve its inhibition to collagen accumulation while reducing compounds toxicity.

By means of a series of chemical modifications, we got four highly active and low toxic compounds: **5c**, **5k**, **9d**, and **9g**. Taken together, the results above encouraged us to further measure IC₅₀ of the four compounds. Their screening data were depicted in Table 3.

Table 3. IC₅₀ values against TGF- β -induced total collagen accumulation in NRK-49F cells.

Compds	IC ₅₀ (μ M)	Compds	IC ₅₀ (μ M)
5c	3.96 \pm 0.31	5k	4.35 \pm 0.31
9d	4.31 \pm 0.35	9g	3.71 \pm 0.22
Nintedanib	1.10 \pm 0.13		

The results are the means \pm SD of at least three independent experiments.

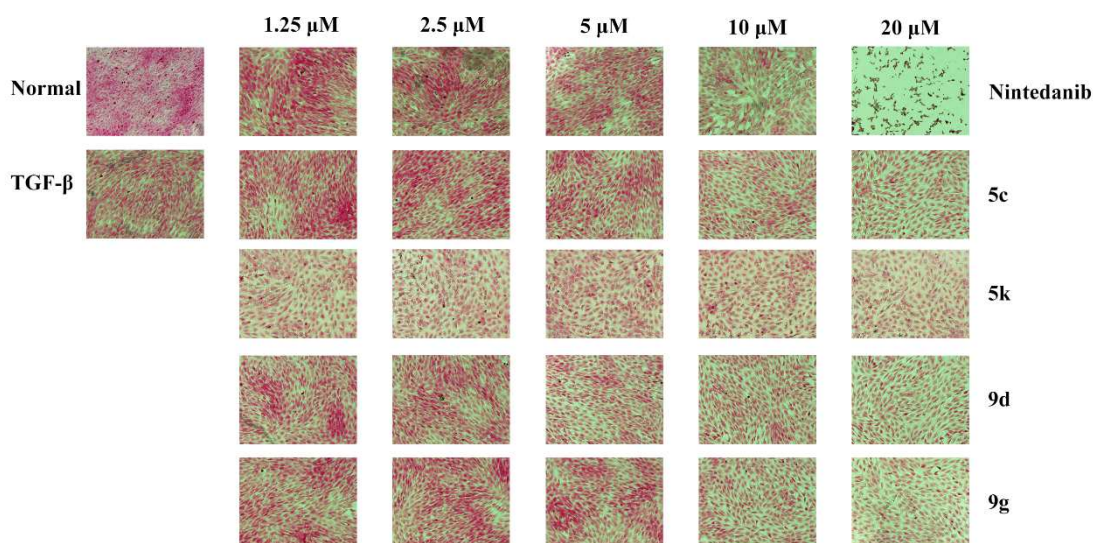


Figure 3. Picro-Sirius red (PSR) staining for the change of TGF- β -induced total collagen accumulation in NRK-49F cells.

The visible mode of extracellular collagen deposition was established upon Picro-Sirius red (PSR) staining to test inhibitory activity of **5c**, **5k**, **9d**, and **9g** against TGF- β -induced total collagen accumulation. As shown in Figure 3, treatment with **5c**, **5k**, **9d**, and **9g** alleviated the total collagen accumulation in a dose-dependent manner. It was proved that the four compounds do have potential effect on inhibiting the production of collagen in vitro.

2.2.2 Inhibition by fibroblasts-driven macrophage migration in vitro.

Macrophages play an important role in the occurrence and progression of fibrosis [27]. Macrophages are recruited to the lesions, and then differentiate to proliferate to form local macrophages, which infiltrate and secrete differently.

Inflammatory mediators cause aggravation of inflammation and promote fibrosis, and migration of macrophages is particularly important for the above processes. We further developed in vitro model to study fibroblasts-induced macrophage migration and activation.

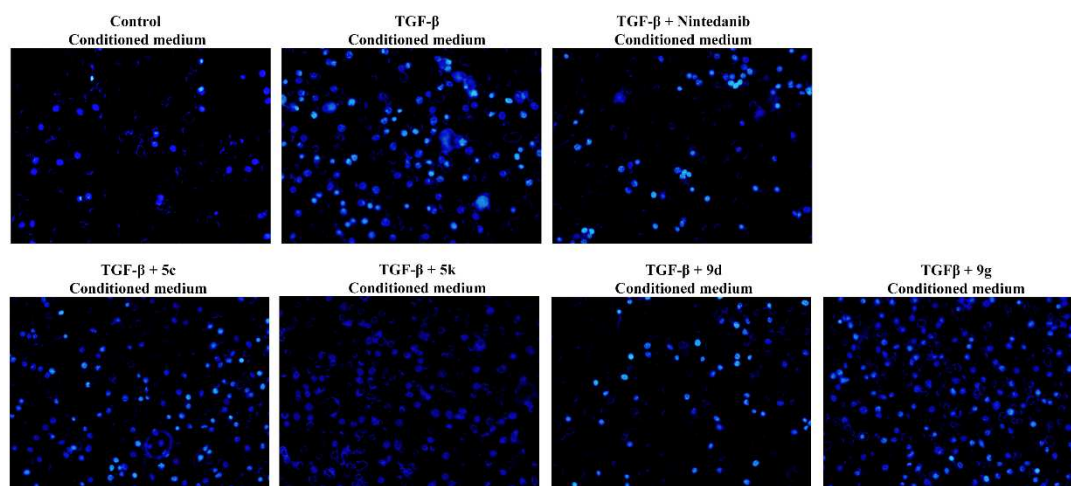


Figure 4. Effect of compounds on fibroblasts-driven macrophage migration in vitro. Representative images and Quantitative analysis (expressed as % macrophage migration) of DAPI stained migrated mouse RAW macrophages (seeded on the upper chamber on the transwell inserts) in response to non-cell treated control medium (control), conditioned medium from NIN3T3 cells that are treated with TGF- β (5 ng/ml) with or without 1 μ M different compounds in the lower chamber.

As shown in Figure 4, the four compounds **5c**, **5k**, **9d** and **9g** had different degrees of inhibition on macrophage migration at a concentration of 1 μ M compared to the control group treated with only TGF- β , with compound **9d** being the most active. Macrophage migration is important for the formation of local macrophages,

secretion of cytokines, promotion of local inflammatory response, and aggravation of fibrosis. This experiment further confirmed that the four compounds have anti-inflammatory and anti-fibrotic effects in vitro. In summary, compound **9d** was selected as a potential drug candidates for follow-up research.

2.2.3 *9d* suppressed the TGF- β 1-induced protein expression of COL1A1, α -SMA, and p-Smad3 in vitro.

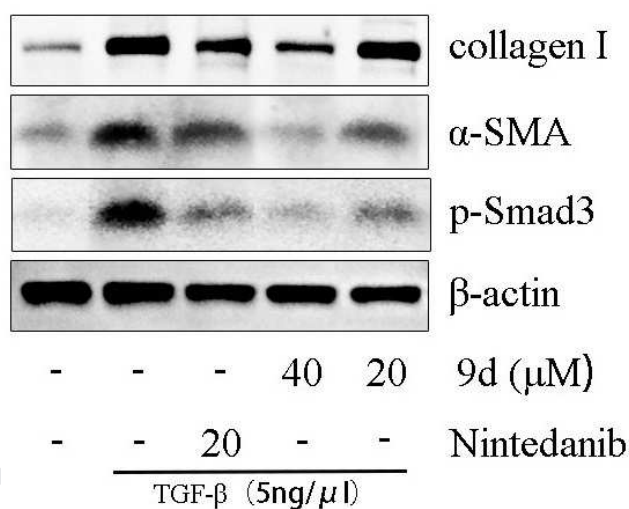


Figure 5. Protein expression levels of COL1A1, α -SMA, and Smad3 were probed through western blot. NRK-49F cells were treated with/without TGF- β (5 ng/mL) and compound **9d** (20 and 40 μ M) for 24 h. The expression of α -SMA, CoL1A1 were examined by Western blot. NRK-49F cells were treated with/without TGF- β (5 ng/mL) and compound **9d** (20 and 40 μ M) for 30min, the expression of p-Smad3 was examined by Western blot. β -Actin was used as a loading control.

Collagen type I alpha 1 (COL1A1), α -smooth muscle actin (α -SMA) overexpressed in fibrotic diseases, which have been commonly considered as fibrotic markers. To further investigate the anti-fibrotic activity of compound **9d**, their abilities of suppressing protein expression of COL1A1, α -SMA in vitro were investigated. TGF- β binds to its receptor and recruits downstream Smad3 proteins to cause the differentiation of quiescent fibroblasts into ECM-secreting myofibroblasts. Therefore, TGF- β /Smad3 pathway has been the target of many attempts in fibrosis [28]. It was obviously in Figure 5 to observe that **9d** could decrease TGF- β -induced COL1A1 and α -SMA expression in NRK-49F cells, which means ECM deposition was also reduced. In addition, much lower phosphorylation levels of Smad3 indicated that **9d** perhaps inhibited TGF- β /Smad3 pathway to ameliorate fibrotic degree.

2.2.4 Pharmacokinetic experiment

In rat pharmacokinetic study (Table 4), **9d** exhibited reasonable maximum concentration ($C_{\max} = 74.73 \mu\text{g/L}$), acceptable oral clearance rate ($Cl = 6.45 \text{ L/h/kg}$), favorable half-life ($t_{1/2} = 13.09 \text{ h}$) and good bioavailability ($F = 39.88\%$) at an oral dose of 10 mg/kg, which is much better than the oral bioavailability of **Nintedanib** ($F = 12\%$ in rats).

Table 4. Pharmacokinetic parameters for compounds **9d** in SD rat

Compound	9d	
	intravenous injection	oral administration
dose (mg/kg)	5	10

C_{\max} ($\mu\text{g/L}$)	316.44	74.73
t_{\max} (h)	2.68	0.63
$t_{1/2}$ (h)	7.42	13.09
AUC_{0-t} ($\mu\text{g/L}\cdot\text{h}$)	1385.24	1104.95
F%		39.88

Data were mean concentrations in rat plasma (n = 5).

2.2.5 Pulmonary fibrosis model induced by bleomycin in vivo

Pulmonary fibrosis is a long-term, progressive pulmonary disease accompanied with excessive deposition of extracellular matrix, which was composed of collagen, fibronectin and other inflammatory cells [29]. To search anti-fibrotic potencies of **9d** in vivo, bleomycin induced lung fibrosis model was employed [30, 31]. **Nintedanib** was administered orally respectively at the dose of 50 mg/kg/day after the bleomycin injection as a positive medicine. Compound **9d** also was administered orally respectively at the dose of 50 and 100 mg/kg/day.

Hydroxyproline is one of the biomarkers of collagen, so it was measured on the 14th and 28th day of administration. Hydroxyproline contents in model group at day 14 and 28 shows significantly increased compared to sham group, which means bleomycin induced lung fibrosis model was successful established. **Nintedanib** group distinguish with sham group at day 28, and long-term medication may reduce the degree of fibrosis. The in vivo effect of inhibiting fibrosis between Compound **9d** and **Nintedanib** group is not obvious at the dose of 50 mg/kg/day. However, Compound **9d** at the dose of 100 mg/kg/day indicated a better therapeutic effect because of its lower hydroxyproline content (Figure 6A). Additionally, the survival

rate of **9d** at both doses (50 mg/kg/day and 100 mg/kg/day) was about 90%, which was better than **Nintedanib** group and model group, suggesting **9d** possessed lower toxicity and better efficacy in the treatment of pulmonary fibrosis.

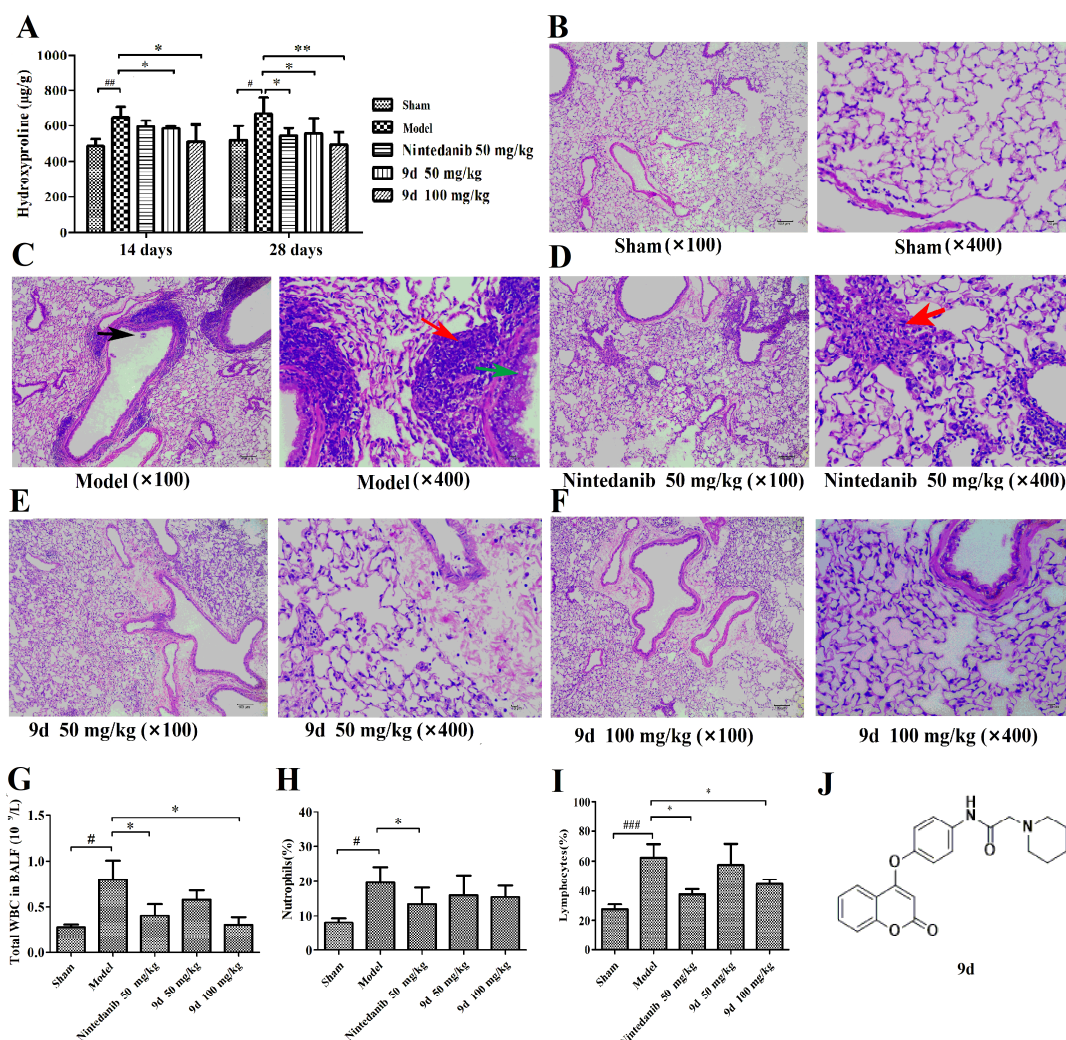


Figure 6. In vivo effects of compounds **9d** on bleomycin-induced pulmonary fibrosis in mice.

C57BL/6 male mice were intratracheal instilled with BLM (2 U/kg) to induce pulmonary fibrosis. Compounds **9d** and **Nintedanib** were given orally once daily after BLM treatment and lungs were harvested at day 14 and day 28 for the following analysis (n = 10 per group). (A) Hydroxyproline contents in lung tissues of each group were measured at day 14 and 28 as described in the methods (*P < 0.05, **P < 0.01). (B-F) 28 days after BLM instillation, lung

tissues of each group mice were measured by hematoxylin-eosin (H&E) (100X & 400X). (↓) Bronchiolar epithelial cell shedding; (↓) Bronchioles and perivascular inflammatory cell infiltration; (↓) Bronchial epithelial vacuolar degeneration. (G-I) Inflammatory cells accounted for the white blood cell in broncho alveolar lavage fluid. (*p < 0.05) (G) Total white blood cells in each group after administration of 28 days. (H) Neutrophils in WBC and (I) Lymphocytes in WBC. (J) Structure of compound **9d**.

The sections of the sham group displayed clear lung structures that the bronchial ciliated epithelium was neatly arranged, and the bronchial and perivascular interstitial were hardly edematous. In contrast, the alveolar structures were destroyed in the model group. It is clear to observe the degeneration and necrosis of bronchial epithelial cells (Figure 6C, ↓ & ↓). There are a number of inflammatory cell infiltration in the alveolar interstitial, mainly lymphocytes and neutrophils (↓). Compound treatments (**Nintedanib** group and **9d** group) delayed the reduction of the number of alveoli and destruction of alveolar structures. In the vicinity of the pulmonary artery, the inflammatory cell infiltration in the drug treatment group was also reduced, especially in **9d** group at 100 mg/kg (Figure 6F).

Inflammation aggravating fibrosis in airway, and the airway wall is mainly dominated by macrophages and lymphocytes, while macrophages and neutrophils play important roles in the lumen. Inflammatory cells such as leukocytes, lymphocytes and neutrophils were documented to act importantly in response to lung fibrotic reactions. To evaluate effects of **9d** on the airway inflammation in mice, we

checked the amount of inflammatory cells in broncho alveolar lavage fluid (BALF) in day 28, which also determined the degree of inflammation caused by bleomycin. Compared with the sham group (Figure 6G-I), the number of total white blood cells in model group is 0.80×10^9 /L that consist of 13.41% for neutrophils, 62.28% for lymphocytes. **9d** can greatly reduce the percentage of inflammatory cells in broncho alveolar lavage fluid at 100 mg/kg (0.30×10^9 /L for total WBC number, 15.49% for neutrophils, and 44.71% for lymphocytes). Meantime, cell composition of **Nintedanib** group at 50 mg/kg (0.41×10^9 /L for total WBC number, 19.70% for neutrophils, and 37.55% for lymphocytes) was similar to compound **9d** group at 100 mg/kg, which suggest that **9d** could effectively reduce inflammatory cell infiltration in BALF at high dose.

To sum up, compound **9d** showed low toxicity and high survival rate in mice in a 28-day dosing regimen. Additional, **9d** obviously reduced collagen deposition in lung tissue and ameliorate inflammatory condition by decrease total number of WBC and other inflammatory cells (especially lymphocytes) in BALF in the lung fibrosis model in vivo. Therefore, compound **9d** can be used as a potential effective compound for anti-fibrosis in vivo by oral administration.

3. Conclusion

In this study, 30 novel compounds bearing coumarin scaffold were synthesized and evaluated for their anti-fibrosis, anti-migration of macrophages in vitro. Among them, compound **9d** showed potent anti-fibrosis abilities in inhibiting TGF- β -induced

total collagen accumulation in NRK-49F cells with low toxicity and migration of macrophages. **9d** was also observed to suppress the TGF- β 1-induced protein expression of COL1A1, α -SMA, and p-Smad3 in vitro by western blot analysis, which indicated TGF- β /Smad3 signaling pathway was inhibited to reduce ECM. In addition, compound **9d** attenuated bleomycin-induced pulmonary fibrosis in mice by reducing hydroxyproline content and inflammatory cell infiltration in lung tissue, which may be related to its inhibition of TGF- β pathway and anti-inflammatory. Considering its extensive structural sources, good pharmacokinetic characteristics (F = 39.88%), anti-fibrotic treatment and low toxicity in vivo, compound **9d** could be a promising, potential, orally active candidate for the treatment of fibrotic disease.

4. Experimental

4.1 Chemistry.

All the chemical solvents and reagents used in this study were analytically pure without further purification and commercially available. TLC was performed on 0.20 mm silica gel 60 F₂₅₄ plates (Qingdao Ocean Chemical Factory, Shandong, China). Visualization of spots on TLC plates was done by UV light and I₂. NMR data were measured for ¹H at 400 MHz and for ¹³C at 101 MHz on a Bruker Avance 400 spectrometer (Bruker Company, Germany) using TMS as an internal standard. Mass spectra (MS) were obtained by Q-TOF Premier mass spectrometer (Micromass, Manchester, UK).

Procedure for synthesis of compound 1b

A solution of 1-(2-hydroxy-4-methoxyphenyl)ethan-1-one (1.0 equiv) in appropriate amount of diethylcarbonate was added dropwise to a oven-dried round bottom flask containing sodium hydride (5.0 equiv) in equal amount of diethylcarbonate at 0°C. After complete addition, the reaction mixture was stirred at 0°C for 30 min and refluxed for three more hours at 100°C. After the reaction was over monitored by TLC, the reaction mixture was cooled to room temperature and ice water was added slowly to quench the reaction mixture. Then use a large amount of ether to wash away diethylcarbonate. After that, the aqueous phase was acidized to pH 3-4 with diluted hydrochloric acid solution to form white solid. Finally the pure light white precipitate was collected by filtration, washed with water, and dried in vacuum to obtain **1b**. ¹H NMR (400 MHz, DMSO-d₆) δ: 12.37 (s, 1H), 7.72 (d, *J* = 8.6 Hz, 1H), 6.93 (m, 2H), 5.47 (s, 1H), 3.86 (s, 3H). MS (ESI), *m/z*: 193.04 [M + H]⁺.

Procedure for synthesis of compound 1c

The sodium nitrate (1.0 equiv) in concentrated sulfuric acid stirred at 0°C, 1a (1.0 equiv) being added. Kept the temperature stirring for 1 h. Ended reaction via TLC monitoring. Slowly added crushed ice under low temperature, then filtrated and dried under vacuum to obtain **1c**. ¹H NMR (400 MHz, DMSO-d₆) δ: 8.53 (d, *J* = 2.6 Hz, 1H), 8.45 (dd, *J* = 9.1, 2.7 Hz, 1H), 7.63 (dd, *J* = 17.8, 8.2 Hz, 1H), 5.71 (s, 1H). MS (ESI), *m/z*: 208.02 [M + H]⁺.

General procedure for synthesis of compounds 2a, 2b and 2c

An appropriate amount of **1a(1b, 1c)** (1.0 equiv) was dissolved in freshly distilled acetonitrile in a oven-dried round bottom flask at room temperature. TBAB (1.5 equiv) was added randomly in one time. Then the reaction was moved to heating and refluxed at 100°C. P₂O₅ (2.4 equiv) was added in batches. Kept the temperature for more than four hours and monitored the reaction by TLC. Then the solvent was removed in vacuum. Added little amount of water to the oil-like compound. Then the aqueous layer was extracted with ethyl acetate three times. The combined organic layer was washed with brine and dried over Na₂SO₄. Finally, the solvent was removed by evaporation to obtain light yellow solid **2a(2b, 2c)**.

4-bromo-2H-chromen-2-one (2a). ¹H NMR (400 MHz, DMSO-d₆) δ: 6.9 (s, 1H), 7.29 (m, 1H), 7.4 (m, 2H), 7.80 (m, 1H). MS (ESI), m/z: 224.95 [M + H]⁺.

4-bromo-7-methoxy-2H-chromen-2-one (2b). ¹H NMR (400 MHz, DMSO) δ 7.72 – 7.67 (m, 1H), 7.02 (dd, *J* = 7.5, 2.2 Hz, 2H), 6.87 (s, 1H), 3.88 (s, 3H). MS (ESI), m/z: 254.94 [M + H]⁺.

4-bromo-6-nitro-2H-chromen-2-one (2c). ¹H NMR (400 MHz, DMSO) δ 8.63 (d, *J* = 2.9 Hz, 1H), 8.34 (dd, *J* = 9.0, 2.9 Hz, 1H), 7.43 (d, *J* = 9.0 Hz, 1H); 7.43 (d, *J* = 9.0 Hz, 1H). MS (ESI), m/z: 269.03 [M + H]⁺.

General procedure for synthesis of compounds 3a, 3b, 3c and 3d

An appropriate amount of **2a(2b, 2c)** (1.0 equiv) and p-phenylenediamine or 2-fluorobenzene-1,4-diamine (1.1 equiv) were dissolved in ethanol in a oven-dried round bottom flask. Et₃N (1.0 equiv) was added to the reaction mixture. The reaction mixture was kept at 70°C for 2 h and then stirred at room temperature for further 4 h.

The crude product was recrystallized from ethanol to obtain a white solid **3a**(**3b**, **3c**, **3d**).

4-((4-aminophenyl)amino)-2H-chromen-2-one (3a). ^1H NMR (400 MHz, DMSO- d_6) δ : 9.06 (s, 1H), 8.21 (d, $J = 7.5$ Hz, 1H), 7.63 (t, $J = 7.3$ Hz, 1H), 7.35 (m, 2H), 6.99 (d, $J = 8.5$ Hz, 2H), 6.66 (d, $J = 8.5$ Hz, 2H), 5.23 (s, 2H), 5.00 (s, 1H). MS (ESI), m/z : 253.09 $[\text{M} + \text{H}]^+$.

4-((4-amino-3-fluorophenyl)amino)-2H-chromen-2-one (3b). ^1H NMR (400 MHz, DMSO- d_6) δ : 9.11 (s, 1H), 8.19 (d, $J = 7.8$ Hz, 1H), 7.64 (t, $J = 7.6$ Hz, 1H), 7.37 (dd, $J = 10.9, 8.3$ Hz, 2H), 7.04 (d, $J = 12.0$ Hz, 1H), 6.87 (m, 2H), 5.28 (s, 2H), 5.07 (s, 1H). MS (ESI), m/z : 271.08 $[\text{M} + \text{H}]^+$.

4-((4-aminophenyl)amino)-7-methoxy-2H-chromen-2-one (3c). ^1H NMR (400 MHz, DMSO- d_6) δ : 1H NMR (400 MHz, DMSO) δ 8.96 (s, 1H), 8.11 (d, $J = 9.0$ Hz, 1H), 6.96 (m, 3H), 6.90 (d, $J = 2.5$ Hz, 1H), 6.64 (m, 2H), 5.21 (s, 2H), 4.87 (s, 1H), 3.86 (s, 3H). MS (ESI), m/z : 283.10 $[\text{M} + \text{H}]^+$.

4-((4-aminophenyl)amino)-6-nitro-2H-chromen-2-one (3d). ^1H NMR (400 MHz, DMSO- d_6) δ : 9.52 (s, 1H), 9.28 (d, $J = 2.1$ Hz, 1H), 8.45 (dd, $J = 9.1, 2.2$ Hz, 1H), 7.57 (d, $J = 9.1$ Hz, 1H), 7.00 (d, $J = 8.4$ Hz, 2H), 6.67 (d, $J = 8.4$ Hz, 2H), 5.27 (s, 2H), 5.12 (s, 1H). MS (ESI), m/z : 298.07 $[\text{M} + \text{H}]^+$.

General procedure for synthesis of compound 6

A solution of **2a** (1.0 equiv), p-nitrophenol (1.5 equiv) and K_2CO_3 (1.8 equiv) in acetone in a oven-dried round bottom flask was heated to 65°C and stirred for 24 h. After the reaction was over monitored by TLC, the solvent was removed by

evaporation to get a kind of yellow solid. Water was added into the solid and then extracted with ethyl acetate three times, washed with brine and dried over Na₂SO₄. The solvent was removed in vacuum to get crude yellow solid and then the residue was purified by recrystallization from ethanol to obtain a light yellow product **6**.

4-(4-nitrophenoxy)-2H-chromen-2-one (6a). ¹H NMR (400 MHz, DMSO-d₆) δ: 8.41 (m, 2H), 8.01 (dd, *J* = 7.9, 1.4 Hz, 1H), 7.77 (m, 1H), 7.68 (m, 2H), 7.48 (m, 2H), 5.53 (s, 1H). MS (ESI), *m/z*: 284.05 [M + H]⁺.

7-methoxy-4-(4-nitrophenoxy)-2H-chromen-2-one (6b). ¹H NMR (400 MHz, DMSO-d₆) δ: 8.39 (m, 2H), 7.90 (d, *J* = 8.8 Hz, 1H), 7.65 (m, 2H), 7.11 (d, *J* = 2.4 Hz, 1H), 7.05 (dd, *J* = 8.8, 2.4 Hz, 1H), 5.35 (s, 1H), 3.90 (s, 3H). MS (ESI), *m/z*: 314.02 [M + H]⁺.

General procedure for synthesis of compound 7

Compound **6** was dissolved in methanol in a oven-dried three-neck round bottom flask with little amount of palladium as a catalyst and hydrogenated for over three hours at room temperature. After the reaction was over, the catalyst was filtered off and the solvent was removed by evaporation to get a brown solid which was then dried at 70 °C under vacuum to obtain **7**.

4-(4-aminophenoxy)-2H-chromen-2-one (7a). ¹H NMR (400 MHz, DMSO-d₆) δ: 8.01 (d, *J* = 7.0 Hz, 1H), 7.74 (dd, *J* = 11.4, 4.2 Hz, 1H), 7.45 (dd, *J* = 12.7, 7.9 Hz, 2H), 6.98 (d, *J* = 8.7 Hz, 2H), 6.70 (m, 2H), 5.26 (s, 2H), 5.18 (s, 1H). MS (ESI), *m/z*: 254.07 [M + H]⁺.

4-(4-aminophenoxy)-7-methoxy-2H-chromen-2-one (7b). ^1H NMR (400 MHz, DMSO- d_6) δ : 7.90 (d, $J = 8.8$ Hz, 1H), 7.02 (m, 2H), 7.01 (m, 2H), 6.61 (m, 2H), 5.24 (s, 2H), 5.01 (s, 1H), 3.95 (m, 3H). MS (ESI), m/z : 284.08 $[\text{M} + \text{H}]^+$.

General procedure for synthesis of compounds 4a, 4b, 4c, 4d and 8a, 8b.

Chloroacetyl chloride (1.2 equiv) was added dropwise to a mixture of the appropriate aromatic amine (1.0 equiv) and triethylamine (1.5 equiv) in freshly distilled DMF in a oven-dried round bottom flask at 0-5°C for 1 h and at room temperature for further 2 h. It was then poured into crushed ice to form a white solid which was filtered, washed with little amount of ethanol and dried under vacuum to obtain **4a**, **4b**, **4c**, **4d**, **8**, respectively.

2-chloro-N-(4-((2-oxo-2H-chromen-4-yl)amino)phenyl)acetamide (4a). ^1H NMR (400 MHz, DMSO- d_6) δ : 10.44 (s, 1H), 9.28 (s, 1H), 8.24 (d, $J = 7.7$ Hz, 1H), 7.68 (m, 3H), 7.38 (m, 4H), 5.24 (s, 1H), 4.28 (s, 2H). MS (ESI), m/z : 329.06 $[\text{M} + \text{H}]^+$.

2-chloro-N-(2-fluoro-4-((2-oxo-2H-chromen-4-yl)amino)phenyl)acetamide (4b). ^1H NMR (400 MHz, DMSO- d_6) δ : 10.17 (s, 1H), 9.33 (s, 1H), 8.21 (d, $J = 7.6$ Hz, 1H), 7.96 (t, $J = 8.7$ Hz, 1H), 7.67 (t, $J = 7.4$ Hz, 1H), 7.39 (m, 3H), 7.24 (d, $J = 8.8$ Hz, 1H), 5.41 (s, 1H), 4.37 (s, 2H). MS (ESI), m/z : 347.05 $[\text{M} + \text{H}]^+$.

2-chloro-N-(4-((7-methoxy-2-oxo-2H-chromen-4-yl)amino)phenyl)acetamide (4c). ^1H NMR (400 MHz, DMSO- d_6) δ : 10.42 (s, 1H), 9.19 (s, 1H), 8.14 (d, $J = 9.0$ Hz, 1H), 7.70 (d, $J = 8.8$ Hz, 2H), 7.33 (d, $J = 8.8$ Hz, 2H), 6.99 (dd, $J = 8.9, 2.5$ Hz, 1H), 6.94 (d, $J = 2.5$ Hz, 1H), 5.11 (s, 1H), 4.27 (s, 2H), 3.87 (s, 3H). MS (ESI), m/z : 359.07 $[\text{M} + \text{H}]^+$.

2-chloro-N-(4-((6-nitro-2-oxo-2H-chromen-4-yl)amino)phenyl)acetamide (4d).

¹H NMR (400 MHz, DMSO-d₆) δ: 10.45 (s, 1H), 9.74 (s, 1H), 9.31 (d, *J* = 2.5 Hz, 1H), 8.48 (dd, *J* = 9.1, 2.6 Hz, 1H), 7.73 (d, *J* = 8.8 Hz, 2H), 7.61 (d, *J* = 9.1 Hz, 1H), 7.37 (d, *J* = 8.8 Hz, 2H), 5.35 (s, 1H), 4.28 (s, 2H). MS (ESI), *m/z*: 374.05 [M + H]⁺.

2-chloro-N-(4-((2-oxo-2H-chromen-4-yl)oxy)phenyl)acetamide (8a). ¹H NMR (400 MHz, DMSO-d₆) δ: 10.59 (s, 1H), 8.04 (d, *J* = 7.8 Hz, 1H), 7.76 (dd, *J* = 16.1, 8.5 Hz, 3H), 7.47 (m, 2H), 7.35 (m, 2H), 5.22 (s, 1H), 4.31 (s, 2H). MS (ESI), *m/z*: 330.05 [M + H]⁺.

2-chloro-N-(4-((7-methoxy-2-oxo-2H-chromen-4-yl)oxy)phenyl)acetamide (8b). ¹H NMR (400 MHz, DMSO-d₆) δ: 10.49 (s, 1H), 7.94 (d, *J* = 8.8 Hz, 1H), 7.75 (d, *J* = 8.8 Hz, 2H), 7.33 (d, *J* = 8.8 Hz, 2H), 7.05 (m, 2H), 5.05 (s, 1H), 4.29 (s, 2H), 3.89 (s, 3H). MS (ESI), *m/z*: 360.06 [M + H]⁺.

General procedure for synthesis of the final products by means of substitution (5a-5t and 9a-9j).

Different acetyl chloride derivatives (1.0 equiv) with catalytic equivalent KI was dissolved in freshly distilled DMF in a oven-dried round bottom flask. Different aliphatic amines (3.0 equiv) was added dropwise. The reaction mixture was stirred at room temperature for 3 h. After the reaction monitored by TLC was over, the reaction mixture was poured into water, extracted with ethyl acetate three times, washed with brine and dried over Na₂SO₄. The solvent was removed by evaporation. The crude residue was purified by chromatography on silica gel to obtain the final products.

*2-(4-methylpiperazin-1-yl)-N-(4-((2-oxo-2H-chromen-4-yl)amino)phenyl)**aceta-mide (5a).*

5a is a white solid, yield 80%. Melting point: 283.7 ± 2.26 °C. ^1H NMR (400 MHz, DMSO) δ 9.92 (s, 1H), 9.41 (d, $J = 6.5$ Hz, 1H), 8.32 (d, $J = 8.0$ Hz, 1H), 7.77 (dd, $J = 14.6, 8.7$ Hz, 2H), 7.66 (t, $J = 7.3$ Hz, 1H), 7.35 (dd, $J = 12.7, 10.5, 5.9$ Hz, 4H), 5.21 (s, 1H), 3.15 (s, 2H), 2.55 (s, 4H), 2.42 (s, 4H), 2.20 (s, 3H). ^{13}C NMR (101 MHz, DMSO) δ 168.33, 161.97, 153.82, 153.23, 136.99, 133.77, 132.85, 126.26, 124.08, 123.25, 120.93, 117.50, 114.89, 84.45, 60.60, 53.33, 51.66, 50.00. MS (ESI), m/z : 393.18 $[\text{M} + \text{H}]^+$

2-morpholino-N-(4-((2-oxo-2H-chromen-4-yl)amino)phenyl)acetamide(5b).

5b is a white solid, yield 89%. Melting point: 244.25 ± 3.05 °C. ^1H NMR (400 MHz, DMSO) δ 9.87 (s, 1H), 9.27 (s, 1H), 8.24 (d, $J = 7.3$ Hz, 1H), 7.75 (d, $J = 8.8$ Hz, 2H), 7.66 (m, 1H), 7.39 (dd, $J = 13.1, 7.8$ Hz, 2H), 7.32 (d, $J = 8.8$ Hz, 2H), 5.21 (s, 1H), 3.65 (m, 4H), 3.15 (s, 2H), 2.53 (m, 4H). ^{13}C NMR (101 MHz, DMSO) δ 168.61, 161.91, 153.87, 153.21, 137.11, 133.71, 132.79, 126.23, 124.03, 123.20, 120.91, 117.51, 114.94, 100.00, 84.46, 66.57, 62.54, 53.67. MS (ESI), m/z : 380.15 $[\text{M} + \text{H}]^+$

*2-((S)-3-methylpiperidin-1-yl)-N-(4-((2-oxo-2H-chromen-4-yl)amino)phenyl)**aceta-mide(5c).*

5c is a white solid, yield 89%. Melting point: 225.15 ± 1.34 °C. ^1H NMR (400 MHz, DMSO) δ 9.78 (s, 1H), 9.27 (s, 1H), 8.24 (d, $J = 7.2$ Hz, 1H), 7.76 (d, $J = 8.8$ Hz, 2H), 7.70 – 7.63 (m, 1H), 7.39 (dd, $J = 13.1, 7.8$ Hz, 2H), 7.32 (d, $J = 8.8$ Hz,

2H), 5.22 (s, 1H), 3.10 (s, 2H), 2.79 (t, $J = 8.8$ Hz, 2H), 2.08 (d, $J = 3.5$ Hz, 1H), 1.79 – 1.52 (m, 5H), 0.85 (d, $J = 6.3$ Hz, 4H). ^{13}C NMR (101 MHz, DMSO) δ 169.12, 161.91, 153.87, 153.21, 137.10, 133.66, 132.80, 126.25, 124.03, 123.20, 120.77, 117.51, 114.94, 84.45, 62.87, 61.88, 54.03, 40.65, 40.44, 40.23, 40.02, 39.81, 39.60, 39.40, 32.58, 30.98, 25.37, 19.91. MS (ESI), m/z : 392.19 $[\text{M} + \text{H}]^+$

N-(4-((2-oxo-2H-chromen-4-yl)amino)phenyl)-2-(piperidin-1-yl)acetamide (**5d**).

5d is a white solid, yield 89%. Melting point: 242.3 ± 1.98 °C. ^1H NMR (400 MHz, DMSO) δ 9.79 (s, 1H), 9.27 (s, 1H), 8.24 (d, $J = 7.1$ Hz, 1H), 7.75 (d, $J = 8.8$ Hz, 2H), 7.65 (m, 1H), 7.39 (dd, $J = 13.1, 7.8$ Hz, 2H), 7.32 (d, $J = 8.7$ Hz, 2H), 5.21 (s, 1H), 3.09 (s, 2H), 2.49 (s, 4H), 1.58 (d, $J = 4.8$ Hz, 4H), 1.41 (s, 2H). ^{13}C NMR (101 MHz, DMSO) δ 169.13, 161.91, 153.87, 153.21, 137.10, 133.66, 132.79, 126.24, 124.03, 123.21, 120.80, 117.50, 114.94, 84.45, 63.16, 54.58, 25.94, 24.04. MS (ESI), m/z : 378.19 $[\text{M} + \text{H}]^+$

N-(4-((2-oxo-2H-chromen-4-yl)amino)phenyl)-2-(pyrrolidin-1-yl)acetamide (**5e**).

5e is a white solid, yield 76%. Melting point: 248.65 ± 1.63 °C. ^1H NMR (400 MHz, DMSO) δ 9.83 (s, 1H), 9.26 (s, 1H), 8.24 (d, $J = 7.1$ Hz, 1H), 7.76 (d, $J = 8.8$ Hz, 2H), 7.66 (m, 1H), 7.39 (dd, $J = 13.0, 7.9$ Hz, 2H), 7.31 (d, $J = 8.8$ Hz, 2H), 5.21 (s, 1H), 3.26 (s, 2H), 2.60 (d, $J = 5.5$ Hz, 4H), 1.76 (m, 4H). ^{13}C NMR (101 MHz, DMSO) δ 169.34, 161.91, 153.87, 153.22, 137.27, 133.58, 132.79, 126.21, 124.03, 123.20, 120.86, 117.51, 114.94, 84.43, 60.05, 54.19, 36.06, 23.96. MS (ESI), m/z : 364.16 $[\text{M} + \text{H}]^+$

N-(2-fluoro-4-((2-oxo-2H-chromen-4-yl)amino)phenyl)-2-(4-methylpiperazin-1-yl)acetamide(**5f**).

5f is a yellow solid, yield 65%. Melting point: 259.41 ± 0.99 °C. ¹H NMR (400 MHz, DMSO) δ 9.64 (s, 1H), 9.32 (s, 1H), 8.21 (d, $J = 7.2$ Hz, 1H), 8.11 (t, $J = 8.8$ Hz, 1H), 7.67 (t, $J = 7.8$ Hz, 1H), 7.38 (m, 3H), 7.23 (d, $J = 8.7$ Hz, 1H), 5.36 (s, 1H), 3.17 (d, $J = 10.5$ Hz, 2H), 2.57 (s, 4H), 2.39 (s, 4H), 2.19 (s, 3H). ¹³C NMR (101 MHz, DMSO) δ 168.93, 161.82, 154.69, 153.84, 152.66, 152.26, 135.38, 135.28, 132.90, 124.10, 123.95, 123.59, 123.25, 121.46, 117.52, 114.88, 112.75, 112.54, 85.59, 61.57, 55.29, 53.12, 46.18. MS (ESI), m/z : 411.18[M + H]⁺

N-(2-fluoro-4-((2-oxo-2H-chromen-4-yl)amino)phenyl)-2-morpholinoacetamide (**5g**).

5g is a yellow solid, yield 72%. Melting point: 213.95 ± 2.74 °C. ¹H NMR (400 MHz, DMSO) δ 9.66 (s, 1H), 9.33 (s, 1H), 8.21 (d, $J = 7.6$ Hz, 1H), 8.04 (t, $J = 8.7$ Hz, 1H), 7.67 (t, $J = 7.5$ Hz, 1H), 7.39 (m, 3H), 7.23 (d, $J = 8.4$ Hz, 1H), 5.37 (s, 1H), 3.65 (s, 4H), 3.20 (s, 2H), 2.56 (s, 4H). ¹³C NMR (101 MHz, DMSO) δ 168.79, 161.82, 153.84, 152.65, 135.67, 135.57, 132.92, 124.35, 124.11, 123.96, 123.85, 123.25, 121.38, 117.53, 114.88, 112.78, 112.56, 85.63, 66.76, 61.93, 53.61. MS (ESI), m/z : 398.14[M + H]⁺

N-(2-fluoro-4-((2-oxo-2H-chromen-4-yl)amino)phenyl)-2-((S)-3-methyl-piperidin-1-yl)acetamide(**5h**).

5h is a yellow solid, yield 72%. Melting point: 256.35 ± 2.47 °C. ¹H NMR (400 MHz, DMSO) δ 9.66 (s, 1H), 9.32 (s, 1H), 8.21 (d, $J = 7.7$ Hz, 1H), 8.14 (t, $J = 8.8$

Hz, 1H), 7.67 (t, $J = 7.6$ Hz, 1H), 7.39 (dt, $J = 20.4, 10.1$ Hz, 3H), 7.22 (d, $J = 8.4$ Hz, 1H), 5.36 (s, 1H), 3.13 (s, 2H), 2.80 (d, $J = 9.0$ Hz, 2H), 2.14 (t, $J = 10.3$ Hz, 1H), 1.87 (t, $J = 10.2$ Hz, 1H), 1.67 (s, 3H), 1.56 (s, 1H), 0.87 (d, $J = 6.1$ Hz, 4H). ^{13}C NMR (101 MHz, DMSO) δ 169.26, 161.82, 153.84, 152.68, 135.28, 135.18, 132.91, 124.11, 124.02, 123.35, 123.25, 121.51, 117.53, 114.88, 112.77, 112.56, 85.58, 62.25, 61.76, 54.04, 32.32, 31.32, 25.54, 19.72. MS (ESI), m/z : 410.18[M + H] $^+$

N-(2-fluoro-4-((2-oxo-2H-chromen-4-yl)amino)phenyl)-2-(piperidin-1-yl)acetamide(**5i**).

5i is a yellow solid, yield 64%. Melting point: 258.55 ± 2.76 °C. ^1H NMR (400 MHz, DMSO) δ 9.68 (s, 1H), 9.32 (s, 1H), 8.21 (d, $J = 7.2$ Hz, 1H), 8.12 (t, $J = 8.8$ Hz, 1H), 7.67 (t, $J = 7.8$ Hz, 1H), 7.38 (m, 3H), 7.23 (d, $J = 8.7$ Hz, 1H), 5.36 (s, 1H), 3.13 (s, 2H), 2.50 (s, 4H), 1.58 (m, 4H), 1.43 (d, $J = 5.0$ Hz, 2H). ^{13}C NMR (101 MHz, DMSO) δ 169.24, 166.95, 161.82, 153.84, 152.68, 152.18, 135.31, 135.21, 132.91, 124.11, 124.00, 123.42, 123.25, 121.50, 117.53, 114.89, 112.76, 112.55, 99.99, 85.57, 62.49, 54.55, 26.25, 23.86. MS (ESI), m/z : 396.16[M + H] $^+$

N-(2-fluoro-4-((2-oxo-2H-chromen-4-yl)amino)phenyl)-2-(pyrrolidin-1-yl)acetamide(**5j**).

5j is a yellow solid, yield 82%. Melting point: 249.85 ± 1.34 °C. ^1H NMR (400 MHz, DMSO) δ 9.68 (s, 1H), 9.32 (s, 1H), 8.21 (d, $J = 7.2$ Hz, 1H), 8.12 (t, $J = 8.8$ Hz, 1H), 7.67 (t, $J = 7.8$ Hz, 1H), 7.38 (m, 3H), 7.23 (d, $J = 8.7$ Hz, 1H), 5.36 (s, 1H), 3.13 (s, 2H), 2.50 (s, 4H), 1.58 (m, 4H), 1.43 (d, $J = 5.0$ Hz, 2H). MS (ESI), m/z : 382.15[M + H] $^+$

N-(4-((7-methoxy-2-oxo-2*H*-chromen-4-yl)amino)phenyl)-2-(4-methylpiperazin-1-yl)acetamide (**5k**).

5k is a white solid, yield 75%. Melting point: 193.65 ± 2.76 °C. ¹H NMR (400 MHz, DMSO) δ 9.80 (s, 1H), 9.17 (s, 1H), 8.14 (d, *J* = 9.0 Hz, 1H), 7.73 (d, *J* = 8.8 Hz, 2H), 7.29 (d, *J* = 8.8 Hz, 2H), 6.99 (dd, *J* = 9.0, 2.5 Hz, 1H), 6.94 (d, *J* = 2.5 Hz, 1H), 5.08 (s, 1H), 3.87 (s, 3H), 3.09 (s, 2H), 2.57 (m, 4H), 2.39 (m, 4H), 2.19 (s, 3H). ¹³C NMR (101 MHz, DMSO) δ 168.51, 165.54, 163.61, 159.84, 154.91, 151.58, 136.84, 134.59, 125.63, 120.07, 112.42, 108.08, 101.30, 92.85, 60.66, 56.48, 54.19, 51.62, 44.71. MS (ESI, m/z): 423.20 [M + H]⁺.

N-(4-((7-methoxy-2-oxo-2*H*-chromen-4-yl)amino)phenyl)-2-morpholino-acetamide (**5l**).

5l is a white solid, yield 78%. Melting point: 202.3 ± 1.56 °C. ¹H NMR (400 MHz, DMSO) δ 9.85 (s, 1H), 9.18 (s, 1H), 8.14 (d, *J* = 9.0 Hz, 1H), 7.74 (d, *J* = 8.8 Hz, 2H), 7.30 (d, *J* = 8.8 Hz, 2H), 6.99 (dd, *J* = 8.9, 2.5 Hz, 1H), 6.94 (d, *J* = 2.5 Hz, 1H), 5.08 (s, 1H), 3.87 (s, 3H), 3.65 (m, 4H), 3.15 (s, 2H), 2.53 (d, *J* = 4.6 Hz, 4H). MS (ESI, m/z): 410.10 [M + H]⁺.

N-(4-((7-methoxy-2-oxo-2*H*-chromen-4-yl)amino)phenyl)-2-((*S*)-3-Methylpiperidin-1-yl)acetamide (**5m**).

5m is a white solid, yield 60%. Melting point: 146.8 ± 2.12 °C. ¹H NMR (400 MHz, DMSO) δ 9.72 (s, 1H), 9.61 (s, 1H), 8.09 (d, *J* = 9.4 Hz, 1H), 7.63 (d, *J* = 8.8 Hz, 2H), 7.13 (d, *J* = 8.8 Hz, 2H), 7.01 – 6.93 (m, 2H), 3.88 (s, 3H), 3.08 (s, 2H),

2.76 (dd, $J = 16.0, 8.2$ Hz, 2H), 2.07 (dd, $J = 10.8, 7.6$ Hz, 1H), 1.65 (ddt, $J = 18.2, 15.0, 7.3$ Hz, 5H), 0.85 (d, $J = 6.3$ Hz, 4H). MS (ESI, m/z): 422.20 $[M + H]^+$.

N-(4-((7-methoxy-2-oxo-2H-chromen-4-yl)amino)phenyl)-2-(piperidin-1-yl)acetamide(**5n**).

5n is a white solid, yield 64%. Melting point: 247.15 ± 2.19 °C. ^1H NMR (400 MHz, DMSO) δ 9.77 (s, 1H), 9.17 (s, 1H), 8.14 (d, $J = 9.0$ Hz, 1H), 7.74 (d, $J = 8.8$ Hz, 2H), 7.29 (d, $J = 8.8$ Hz, 2H), 6.99 (dd, $J = 8.9, 2.5$ Hz, 1H), 6.94 (d, $J = 2.5$ Hz, 1H), 5.08 (s, 1H), 3.87 (s, 3H), 3.08 (s, 2H), 2.47 (d, $J = 5.2$ Hz, 4H), 1.57 (dd, $J = 10.9, 5.6$ Hz, 4H), 1.41 (d, $J = 4.9$ Hz, 2H). ^{13}C NMR (101 MHz, DMSO) δ 169.11, 162.95, 162.22, 155.72, 153.45, 136.99, 133.74, 126.19, 124.42, 120.76, 111.86, 108.04, 101.45, 82.40, 63.16, 56.32, 54.57, 25.94, 24.04. MS (ESI, m/z): 408.01 $[M + H]^+$.

N-(4-((7-methoxy-2-oxo-2H-chromen-4-yl)amino)phenyl)-2-(pyrrolidin-1-yl)acetamide(**5o**).

5o is a white solid, yield 52%. Melting point: 186.65 ± 1.34 °C. ^1H NMR (400 MHz, DMSO) δ 9.84 (s, 1H), 9.24 (s, 1H), 8.18 (d, $J = 8.9$ Hz, 1H), 7.81 (d, $J = 8.7$ Hz, 2H), 7.29 (d, $J = 8.7$ Hz, 2H), 6.99 (dd, $J = 9.0, 2.4$ Hz, 1H), 6.93 (d, $J = 2.4$ Hz, 1H), 5.08 (s, 1H), 4.01 (d, $J = 5.9$ Hz, 2H), 3.87 (s, 3H), 2.48 (m, 4H), 1.24 (m, 4H). MS (ESI, m/z): 394.10 $[M + H]^+$.

2-(4-methylpiperazin-1-yl)-*N*-(4-((6-nitro-2-oxo-2H-chromen-4-yl)amino)phenyl)acetamide(**5p**).

5p is a yellow solid, yield 84%. Melting point: 219.20 ± 2.26 . ^1H NMR (400 MHz, DMSO) δ 9.83 (s, 1H), 9.72 (s, 1H), 9.31 (d, $J = 2.2$ Hz, 1H), 8.47 (dd, $J = 9.1$, 2.4 Hz, 1H), 7.76 (d, $J = 8.7$ Hz, 2H), 7.58 (t, $J = 16.5$ Hz, 1H), 7.33 (d, $J = 8.7$ Hz, 2H), 5.33 (s, 1H), 3.12 (d, $J = 15.0$ Hz, 2H), 2.54 (s, 4H), 2.40 (s, 4H), 2.19 (s, 3H). ^{13}C NMR (101 MHz, DMSO) δ 168.82, 160.80, 157.79, 152.22, 143.66, 137.27, 133.22, 127.50, 125.98, 120.84, 120.09, 119.06, 115.52, 84.88, 62.23, 54.97, 53.10, 46.13. MS (ESI), m/z : 438.17[M + H]⁺

2-morpholino-N-(4-((6-nitro-2-oxo-2H-chromen-4-yl)amino)phenyl)acetamide (**5q**).

5q is a yellow solid, yield 85%. Melting point: 248 ± 1.56 . ^1H NMR (400 MHz, DMSO) δ 9.89 (s, 1H), 9.73 (s, 1H), 9.32 (d, $J = 2.5$ Hz, 1H), 8.48 (dd, $J = 9.1$, 2.6 Hz, 1H), 7.77 (d, $J = 8.8$ Hz, 2H), 7.61 (d, $J = 9.1$ Hz, 1H), 7.33 (d, $J = 8.8$ Hz, 2H), 5.33 (s, 1H), 3.65 (m, 4H), 3.16 (s, 2H), 2.51 (s, 4H). ^{13}C NMR (101 MHz, DMSO) δ 168.65, 160.83, 157.81, 152.30, 143.70, 137.30, 133.25, 127.55, 125.99, 120.95, 120.15, 119.09, 115.56, 84.89, 66.57, 62.52, 53.66. MS (ESI), m/z : 425.14[M + H]⁺

2-((S)-3-methylpiperidin-1-yl)-N-(4-((6-nitro-2-oxo-2H-chromen-4-yl)amino)phenyl)acetamide (**5r**).

5r is a yellow solid, yield 67%. Melting point: 256.35 ± 2.47 . ^1H NMR (400 MHz, DMSO) δ 9.81 (s, 1H), 9.73 (s, 1H), 9.32 (d, $J = 2.5$ Hz, 1H), 8.48 (dd, $J = 9.1$, 2.5 Hz, 1H), 7.77 (d, $J = 8.8$ Hz, 2H), 7.60 (d, $J = 9.1$ Hz, 1H), 7.33 (d, $J = 8.8$ Hz, 2H), 5.33 (s, 1H), 3.10 (s, 2H), 2.79 (t, $J = 8.7$ Hz, 2H), 2.08 (d, $J = 3.6$ Hz, 1H), 1.77 – 1.48 (m, 5H), 0.85 (d, $J = 6.3$ Hz, 4H). ^{13}C NMR (101 MHz, DMSO) δ 169.19,

160.85, 157.80, 152.35, 143.69, 137.32, 133.23, 127.52, 125.99, 120.79, 120.31, 119.06, 115.59, 84.83, 62.80, 61.85, 53.99, 32.61, 30.99, 25.39, 19.92. MS (ESI), m/z: 437.17[M + H]⁺

N-(4-((6-nitro-2-oxo-2H-chromen-4-yl)amino)phenyl)-2-(piperidin-1-yl)acetamide(**5s**).

5s is a yellow solid, yield 77%. Melting point: 241.15 ± 2.19 °C. ¹H NMR (400 MHz, DMSO) δ 9.89 (s, 1H), 9.73 (s, 1H), 9.32 (d, *J* = 2.5 Hz, 1H), 8.48 (dd, *J* = 9.1, 2.6 Hz, 1H), 7.77 (d, *J* = 8.8 Hz, 2H), 7.61 (d, *J* = 9.1 Hz, 1H), 7.33 (d, *J* = 8.8 Hz, 2H), 5.32 (s, 1H), 2.50 (s, 4H), 1.58 (m, 4H), 1.43 (d, *J* = 5.0 Hz, 2H). ¹³C NMR (101 MHz, DMSO) δ 169.17, 160.82, 157.82, 152.28, 143.70, 137.28, 133.22, 127.55, 126.01, 120.87, 120.11, 119.10, 115.56, 84.89, 63.16, 54.57, 25.94, 24.04. MS (ESI), m/z: 423.16[M + H]⁺

N-(4-((6-nitro-2-oxo-2H-chromen-4-yl)amino)phenyl)-2-(pyrrolidin-1-yl)acetamide(**5t**).

5t is a yellow solid, yield 76%. Melting point: 288.95 ± 2.47 °C. ¹H NMR (400 MHz, DMSO) δ 9.84 (s, 1H), 9.72 (s, 1H), 9.31 (d, *J* = 2.5 Hz, 1H), 8.48 (dd, *J* = 9.1, 2.5 Hz, 1H), 7.78 (d, *J* = 8.8 Hz, 2H), 7.61 (d, *J* = 9.1 Hz, 1H), 7.32 (d, *J* = 8.8 Hz, 2H), 5.32 (s, 1H), 3.27 (d, *J* = 8.6 Hz, 2H), 2.64 (d, *J* = 26.1 Hz, 4H), 1.76 (t, *J* = 3.4 Hz, 4H). ¹³C NMR (101 MHz, DMSO) δ 169.38, 160.84, 157.83, 152.32, 143.70, 137.43, 133.21, 127.55, 125.97, 120.92, 120.12, 119.10, 115.60, 84.82, 60.05, 54.18, 40.64, 40.43, 40.23, 40.02, 39.81, 39.60, 39.39, 23.96. MS (ESI), m/z: 409.14[M + H]⁺

2-(4-methylpiperazin-1-yl)-N-(4-((2-oxo-2H-chromen-4-yl)oxy)phenyl)acetamide (9a).

9a is a white solid, yield 66% Melting point: 137.05 ± 1.91 °C. ^1H NMR (400 MHz, DMSO) δ 9.89 (s, 1H), 8.04 (m, 1H), 7.77 (m, 3H), 7.47 (dd, $J = 14.2, 7.6$ Hz, 2H), 7.31 (d, $J = 8.9$ Hz, 2H), 5.21 (s, 1H), 3.14 (s, 2H), 2.60 (d, $J = 58.5$ Hz, 4H), 2.39 (s, 4H), 2.18 (s, 3H). ^{13}C NMR (101 MHz, DMSO) δ 168.92, 166.50, 161.61, 153.56, 147.82, 137.68, 133.85, 124.96, 123.47, 121.97, 121.58, 117.06, 115.26, 93.19, 62.24, 54.96, 53.12, 46.16. MS (ESI), m/z : 394.17 $[\text{M} + \text{H}]^+$.

2-morpholino-N-(4-((2-oxo-2H-chromen-4-yl)oxy)phenyl)acetamide (9b).

9b is a white solid, yield 75%. Melting point: 207.23 ± 2.26 °C. ^1H NMR (400 MHz, DMSO) δ 9.94 (s, 1H), 8.04 (dd, $J = 7.9, 1.3$ Hz, 1H), 7.82 (d, $J = 9.0$ Hz, 2H), 7.76 (m, 1H), 7.47 (dd, $J = 14.0, 7.5$ Hz, 2H), 7.32 (d, $J = 9.0$ Hz, 2H), 5.20 (s, 1H), 3.65 (m, 4H), 3.16 (s, 2H), 2.53 (d, $J = 4.6$ Hz, 4H). ^{13}C NMR (101 MHz, DMSO) δ 168.74, 166.51, 161.62, 153.57, 147.87, 137.67, 133.87, 124.99, 123.48, 121.98, 121.68, 117.08, 115.27, 93.21, 66.55, 62.53, 53.66. MS (ESI), m/z : 381.14 $[\text{M} + \text{H}]^+$.

2-((S)-3-methylpiperidin-1-yl)-N-(4-((2-oxo-2H-chromen-4-yl)oxy)phenyl)acetamide (9c).

9c is a white solid, yield 82%. Melting point: 214.95 ± 2.05 °C. ^1H NMR (400 MHz, DMSO) δ 9.85 (s, 1H), 8.04 (dd, $J = 7.9, 1.4$ Hz, 1H), 7.84 – 7.79 (m, 2H), 7.78 – 7.72 (m, 1H), 7.47 (dd, $J = 13.7, 7.5$ Hz, 2H), 7.35 – 7.27 (m, 2H), 5.21 (s, 1H), 3.10 (s, 2H), 2.79 (t, $J = 8.9$ Hz, 2H), 2.07 (td, $J = 10.7, 4.0$ Hz, 1H), 1.75 – 1.50 (m, 5H), 0.85 (d, $J = 6.3$ Hz, 4H). MS (ESI), m/z : 393.17 $[\text{M} + \text{H}]^+$.

N-(4-((2-oxo-2H-chromen-4-yl)oxy)phenyl)-2-(piperidin-1-yl)acetamide(**9d**).

9d is a white solid, yield 87%. Melting point: 219.25 ± 1.91 °C. ¹H NMR (400 MHz, DMSO) δ 9.86 (s, 1H), 8.05 (dd, $J = 7.9, 1.3$ Hz, 1H), 7.77 (m, 3H), 7.48 (dd, $J = 13.7, 7.6$ Hz, 2H), 7.38 (d, $J = 8.8$ Hz, 2H), 5.20 (s, 1H), 4.13 (s, 2H), 3.45 (s, 2H), 3.07 (s, 3H), 1.77 (s, 5H). ¹³C NMR (101 MHz, DMSO): δ 168.26, 166.50, 162.78, 154.20, 151.61, 133.90, 126.92, 123.02, 121.20, 117.08, 115.21, 98.09, 63.46, 51.10, 25.12, 24.54. MS (ESI), m/z : 379.16 [M + H]⁺

N-(4-((2-oxo-2H-chromen-4-yl)oxy)phenyl)-2-(pyrrolidin-1-yl)acetamide(**9e**).

9e is a white solid, yield 65% Melting point: 131.85 ± 2.19 °C. ¹H NMR (400 MHz, DMSO) δ 9.89 (s, 1H), 8.04 (m, 1H), 7.77 (m, 3H), 7.47 (dd, $J = 14.2, 7.6$ Hz, 2H), 7.31 (d, $J = 8.9$ Hz, 2H), 5.20 (s, 1H), 3.14 (s, 2H), 2.60 (d, $J = 5.5$ Hz, 4H), 1.76 (m, 4H). ¹³C NMR (101 MHz, DMSO) δ 161.47, 155.16, 154.27, 131.91, 126.71, 123.46, 117.80, 116.36, 85.66, 52.19, 25.75. MS (ESI), m/z : 365.14 [M + H]⁺.

N-(4-((7-methoxy-2-oxo-2H-chromen-4-yl)oxy)phenyl)-2-(4-methylpiperazin-1-yl)acetamide(**9f**).

9f is a white solid, yield 35%. Melting point: 184.65 ± 2.05 °C. ¹H NMR (400 MHz, DMSO-d₆) δ : 10.03 (s, 1H), 7.98 (d, $J = 8.8$ Hz, 1H), 7.72 (d, $J = 8.9$ Hz, 2H), 7.39 (d, $J = 8.9$ Hz, 2H), 7.05 (m, 2H), 5.02 (s, 1H), 3.89 (s, 3H), 2.60 (d, $J = 58.5$ Hz, 4H), 2.39 (s, 4H), 2.18 (s, 3H). MS (ESI), m/z : 424.18[M + H]⁺.

N-(4-((7-methoxy-2-oxo-2H-chromen-4-yl)oxy)phenyl)-2-morpholinoacetamide(**9g**).

9g is a white solid, yield 35% Melting point: 170.93 ± 2.41 °C. ¹H NMR (400

MHz, DMSO) δ : 9.93 (s, 1H), 7.94 (d, $J = 8.8$ Hz, 1H), 7.80 (d, $J = 8.9$ Hz, 2H), 7.29 (d, $J = 8.9$ Hz, 2H), 7.05 (m, 2H), 5.04 (s, 1H), 3.89 (s, 3H), 3.62 (m, 8H), 3.14 (d, $J = 15.3$ Hz, 2H). MS (ESI), m/z : 411.15[M + H]⁺.

N-(4-((7-methoxy-2-oxo-2H-chromen-4-yl)oxy)phenyl)-2-((S)-3-methyl-piperidin-1-yl)acetamide(**9h**).

9h is a white solid, yield 31%. Melting point: 174.35 ± 2.90 °C. ¹H NMR (400 MHz, DMSO) δ : 9.93 (s, 1H), 7.94 (d, $J = 8.8$ Hz, 1H), 7.80 (d, $J = 8.9$ Hz, 2H), 7.29 (d, $J = 8.9$ Hz, 2H), 7.05 (m, 2H), 5.04 (s, 1H), 3.89 (s, 3H), 3.62 (m, 9H), 3.14 (d, $J = 15.3$ Hz, 3H). MS (ESI), m/z : 423.18[M + H]⁺.

N-(4-((7-methoxy-2-oxo-2H-chromen-4-yl)oxy)phenyl)-2-(piperidin-1-yl)acetamide(**9i**).

9i is a white solid, yield 22%. Melting point: 191.30 ± 2.69 °C. ¹H NMR (400 MHz, DMSO) δ : 9.02 (s, 1H), 7.88 (d, $J = 8.8$ Hz, 1H), 7.76 (d, $J = 8.9$ Hz, 2H), 7.49 (d, $J = 8.9$ Hz, 2H), 7.05 (m, 2H), 5.02 (s, 1H), 3.89 (s, 3H), 3.45 (s, 2H), 3.07 (s, 3H), 1.77 (s, 5H). MS (ESI), m/z : 409.17[M + H]⁺.

N-(4-((7-methoxy-2-oxo-2H-chromen-4-yl)oxy)phenyl)-2-(pyrrolidin-1-yl)acetamide(**9j**).

9j is a white solid, yield 34%. Melting point: 142.85 ± 2.89 °C. ¹H NMR (400 MHz, DMSO) δ : 9.93 (s, 1H), 7.94 (d, $J = 8.8$ Hz, 1H), 7.80 (d, $J = 8.9$ Hz, 2H), 7.29 (d, $J = 8.9$ Hz, 2H), 7.05 (m, 2H), 5.04 (s, 1H), 3.89 (s, 3H), 3.27 (d, $J = 8.6$ Hz, 2H), 2.64 (d, $J = 26.1$ Hz, 4H), 1.76 (t, $J = 3.4$ Hz, 4H). MS (ESI), m/z : 395.15[M + H]⁺.

4.2 Biological.

4.2.1 Total collagen accumulation inhibition *In Vitro*

The anti-fibrosis activities of the compounds were tested in NRK-49F cells. NRK-49 cells were cultured in Dulbecco's Modified Eagle's Medium (DMEM) medium supplemented with 10% fetal bovine serum (FBS) and 1% penicillin-streptomycin in a humidified atmosphere of 5% CO₂ at 37 °C. 8000 cells were plated in 96-well plates in DMEM containing 5% serum. Three days later, replace the supernatant with 1% ITS in no-serum DMEM for other two days. Next the supernatant was removed and the DMEM + 1% ITS medium containing TGF-β (5 ng/ml) and 10 μM compounds to be tested was cultured for last two days. Then remove the supernatant and add 4% paraformaldehyde (100 μl/hole) fixed for thirty minutes in room temperature. Next wash it with PBS twice and added the Sirius red dye (100 μl/hole) with saturated picric acid 4h protecting from light to stain collagenous fiber, which will be dyed red. Then remove the dyeing liquid, add 0.1% acetic acid (100 μl/ hole) to washing three times, dry and photograph under a microscope camera. Last, add 0.1M NaOH (100 μl/ hole), shake and dissolve at room temperature for ten minutes. Determine of each hole OD under wavelength 540 nm to test which compound can inhibit collagen deposition. Total collagen accumulation inhibition = (Administration A value - control A value) / (model A value - control A value) × 100%. All assays were repeated in triplicate.

4.2.2 Cell survival rate measured by MTT assay

The NRK-49F cells were plated in a 96-well plate at a density of 0.5×10^5 cells/ml in a 100 μ l suspension and cultured overnight and the experimental group were added drugs at the concentration of 10 μ M. After 72h, 20 μ l of 5% (m/v) MTT solution was added to each well and incubated for 4 hours in the incubator. Then each well was added 150 μ l DMSO. Finally, the absorbance (A value) of each well was measured on a microplate reader. Survival rate = (Administration A value - Zero A value) / (Blank A value - Zero A value) \times 100%. All assays were repeated in triplicate.

4.2.3 Inhibition Of Macrophage Migration Assay

The transwell migration assay was performed on RAW macrophages using a polycarbonate membrane inserts (8 μ m poresize; Transwell Coster Corning Inc.). The lower chambers were filled with 650 μ l medium (455 μ l of conditioned medium + 175 μ l of fresh medium). The conditioned medium was collected from NIN3T3 cells after different treatment as mentioned above. Cells (1×10^5 cells/100 μ l) were added in the upper chamber (or insert), then incubated at 37 °C for 24 h to allow cell migration through the membrane. After incubation, the chambers were removed and washed twice with PBS and the non-invading cells were discarded using a cotton swab. The cells were fixed in 4% paraformaldehyde, permeabilized in 100% methanol and stained using DAPI nuclear stain. Random selected fields of view were captured.

4.2.4 Western blot Analysis

The protein lysates were harvested using RIPA buffer with 1 mM phenylmethanesulfonyl fluoride (PMSF) and protease inhibitor cocktail, the protein

concentration was determined by a bicinchoninic acid (BCA) kit. Same Proteins (30–40 µg) of each sample were separated on 10%–12% SDS/PAGE gels at 80 V for 20 minutes and then turn to 120V for 1h. And proteins were transferred onto PVDF membranes at 80–100 V for 1 h, membranes were blocked in 5% (wt/vol) dried milk in PBS with 1% Tween 20 and then incubated with the indicated primary antibodies at 4 °C overnight. After incubation with HRP-conjugated secondary antibodies, immunoreactive bands were detected with the SuperLumia ECL Plus HRP Substrate Kit Solution(K22030, ABBKine). Primary antibodies used were:α-SMA(251411, ZENBIO), collagen I(14695-1-AP, proteintech), p-smad3(AF3363, Affinity), GAPDH(AB0037, Abways), secondary antibodies used were: Goat Anti-Rabbit IgG (H+L) HRP(AB0101, Abways), Goat Anti-Mouse IgG (H+L) HRP(AB0102, Abways).

4.2.5 Pharmacokinetic experiment

Sample preparation: Weigh about 15 mg of the test compound, then added 2% Tween 80 and 2% ethanol, and physiological saline to prepare a 1 mg/ml 9d compound solution for administration.

Sample collection: 5 SD rats (Chengdu Dossy Experimental Animal Co., Ltd., license number: SCXK 2015-030) were administered intravenously at 5 mg/kg and 10 mg/kg orally. The drug was administered at 0 min before administration and 5 min, 15 min, 30 min, 1 h, 2 h, 4 h, 6 h, 8 h, 10 h and 24 h after administration, then approximately 0.2 ml of blood was collected, and the collected blood was centrifuged (3500r) for 15 min, and the supernatant plasma was collected at -20 °C for testing.

Sample determination: Preparation the corresponding instruments and equipment: configure the standard solution, accurately pipette a certain amount of the test compound stock solution (1mg/ml) with a pipette, and dilute it to the EP tube with methanol. The concentration is 19.53, 39.06, 78.125, 156.25, 312.5, 625, 1250, 2500, 5000, 10000 ng/ml of the test compound standard solution. Establishment of the standard curve: take 45 μ l of blank plasma in each EP tube, respectively, add 5 μ l of the above each concentration standard solution was vortexed, and 200 μ l of methanol precipitated protein containing 12.5 ng/ml of internal standard SAHA was added, vortexed for 3 min, centrifuged (13,000 rpm, 15 min), and the supernatant was taken 2 μ l. Injection. The theoretical concentrations of the test compounds were 1.95, 3.91, 7.81, 15.63, 31.25, 62.5, 125, 250, 500, 1000 ng/ml; the preparation of plasma samples, the collected plasma samples were thawed at room temperature, and vortexed. Spin and mix evenly. Take 50 μ l of plasma in each EP tube, add 200 μ l of methanol precipitated protein containing 12.5 ng/ml internal standard SAHA, vortex for 3 min, centrifuge (13,000 rpm, 15 min), take 2 μ l for injection analysis; Condition; finally organize the data and calculate the relevant PK value.

4.2.6 BLM-induced animal model of pulmonary fibrosis

Preparation of reagents: (1) Chloral hydrate preparation: Chloral hydrate was prepared into 3% solution. According to the ratio of 1 ml/100 g, the weight of each mouse was 20 g and 200 μ l was injected. (2) Bleomycin preparation: Bleomycin in a bottle of 15 U, first added 5 ml saline to get a liquid with 3 U/ml, and then diluted to 1 U/ml as working fluid. According to the proportion of 3.5 mg/kg, each mouse

weighed about 20 g needed about 75 μ L. 7-8 weeks male C57BL/6 mice were purchased from Chengdu Dossy Experimental Animals CO.,LTD. All mice were acclimatized in a room with constant temperature ($25\pm 2^\circ\text{C}$) and relative humidity ($60\pm 2\%$) and allowed free access to food and water. Specific experimental steps include: (1) Mice were anesthetized using tape affixed them to the anatomical wax and the hair between throat was shaved. (2) Cut off the skin of the larynx and use tweezers to blunt the muscles around the trachea. (3) The trachea was picked out injected with 75 μ l prepared bleomycin solution. (4) Turned the mouse up and down to make bleomycin evenly distributed in the lungs. (5).Finally, sutured the muscle layer and the trachea. Mice were sacrificed at Day 14 and 28. Lung tissue was harvested for the following experiments to evaluate the degree of pulmonary fibrosis.

4.2.7 Hydroxyproline Assay

The collagen contents in right lungs of mice were measured with a conventional Hydroxyproline assay kit (Nanjing Jiancheng Bioengineering Institute, A030-2). In a word, the right lungs were dried and acid hydrolyzed, then the residue was filtered and the PH value was adjusted to 6.5-8.0. The hydroxyproline analysis was performed using chloramine-T spectrophotometric absorbance.

4.2.8 Hematoxylin-Eosin staining (HE staining)

Left lungs were fixed in 10% formalin for 24 h and embedded in paraffin. Then lung sections ($5\mu\text{m}$) were prepared and stained with hematoxylin-eosin staining. HE staining images were collected using an upright transmission fluorescence microscope.

4.2.9 Bronchoalveolar Lavage Fluid Preparation

Bronchoalveolar lavage fluid was prepared by washing the right lungs three times with 1 mL of PBS through a tracheal cannula. Bronchoalveolar lavage fluid sample is sent to West China-Frontier PharmaTech (WCFP) to detect the total number and composition of cells.

Abbreviations

FDA, Food and Drug Administration; EMA, European Medicines Agency; TBAB, tetrabutylammonium bromide; DMF, N, N-Dimethylformamide; MTT, 3-(4,5-dimethylthiazol-2-yl)-2,5-diphenyltetrazolium bromide; ADM, Adriamycin; PTX, paclitaxel; iv, intravenous; ECM, extracellular matrix; Nin, Nintedanib; COL1A1, Collagen type I alpha 1; α -SMA, α -smooth muscle actin; TGF- β , transforming growth factor- β ; p-Smad3, Phospho- Smad3; TNF- α , Tumor Necrosis Factor- α ; IL-6, Interleukin-6; IFN- γ , Interferon- γ ; VEGFR, Vascular Endothelial Growth Factor Receptor 2; PDGFR, Platelet-derived growth factor receptor; FGFR, Fibroblast growth factor receptor-3; ACE-IPF, Anticoagulant Effectiveness in Idiopathic Pulmonary Fibrosis; CML-AGE, N(6)-carboxymethyllysine, soluble receptor for AGEs; CTGF, connective tissue growth factor; SAR, structure activity relationships; SD, Standard Deviation; IC₅₀, Inhibitory concentration 50; BLM, bleomycin; WBC, white blood cell; TLC, thin-layer chromatography; UV, ultraviolet; TMS, Tetramethylsilane; ¹H NMR, nuclear magnetic resonance; MS (ESI), Electrospray ionization mass spectrometry; DMSO, Dimethyl sulfoxide; PBS,

Phosphate buffer; PVDF, polyvinylidene fluoride SAHA, Suberanine hydroxamic acid; PK, pharmacokinetics.

Acknowledgment

The authors greatly appreciate the financial support from Drug Innovation Major Project (2018ZX09711001-002-012), National Natural Science Foundation of China (81702900), and 1.3.5 project for disciplines of excellence, West China Hospital, Sichuan University.

Appendix A. Supplementary data

The ^1H and ^{13}C spectrum of compounds related to this article can be found at **Supplementary data**.

REFERENCES

- [1] Liu Y M , Nepali K , Liou J P . Idiopathic Pulmonary Fibrosis: Current Status, Recent Progress, and Emerging Targets[J]. Journal of Medicinal Chemistry, 2017, 60(2), 527-553.
- [2] Strieter R M , Mehrad B . New Mechanisms of Pulmonary Fibrosis. Chest. 2009, 136(5), 1364-1370.
- [3] Spagnolo P, Sverzellati N, Rossi G, et al. Idiopathic pulmonary fibrosis: an update. Annals of medicine. 2015, 47(1), 15-27.

- [4] Wilson, M. S.; Wynn, T. A. Wilson M S, Wynn T A. Pulmonary fibrosis: pathogenesis, etiology and regulation. *Mucosal immunology*. 2009, 2(2), 103.
- [5] Lederer D J, Martinez F J. Idiopathic Pulmonary Fibrosis.[J]. *N Engl J Med*, 2018, 378(19), 1811-1823.
- [6] King, T. E., Jr; Pardo, A.; Selman, M. Idiopathic pulmonary fibrosis. *Lancet*. 2011, 378, 1949-1961.
- [7] Keane, M. P., D. A. Arenberg, J. P. R. Lynch, R. I. Whyte, M. D. Iannettoni, M. D. Burdick, C. A. Wilke, S. B. Morris, M. C. Glass, B. DiGiovine, et al. The CXC chemokines, IL-8 and IP-10, regulate angiogenic activity in idiopathic pulmonary fibrosis. *Journal of Immunology*. 1997, 159(3), 1437-1443.
- [8] Keane, M. P., J. A. Belperio, T. A. Moore, B. B. Moore, D. A. Arenberg, R. E. Smith, M. D. Burdick, S. L. Kunkel, and R. M. Strieter. Neutralization of the CXC chemokine, macrophage inflammatory protein-2, attenuates bleomycin-induced pulmonary fibrosis. *The Journal of Immunology*. 1999, 162(9), 5511-5518.
- [9] Wynn T A, Barron L. Macrophages: master regulators of inflammation and fibrosis[C]//*Seminars in liver disease*. Thieme Medical Publishers. 2010, 30(03), 245-257.
- [10] Heymann F, Trautwein C, Tacke F. Monocytes and macrophages as cellular targets in liver fibrosis. *Inflammation & Allergy-Drug Targets (Formerly Current Drug Targets-Inflammation & Allergy)*. 2009, 8(4), 307-318.

- [11] Ju C, Tacke F. Hepatic macrophages in homeostasis and liver diseases: from pathogenesis to novel therapeutic strategies. *Cellular & molecular immunology*. 2016, 13(3), 316-327.
- [12] Yukiko Miura, Arata Azuma. Pirfenidone: an orphan drug for treating idiopathic pulmonary fibrosis. *Expert Opinion on Orphan Drugs*. 2015, 3(5):587-597.
- [13] Roth G J, Heckel A, Colbatzky F, et al. Design, synthesis, and evaluation of indolinones as triple angiokinase inhibitors and the discovery of a highly specific 6-methoxycarbonyl-substituted indolinone (BIBF 1120). *Journal of medicinal chemistry*. 2009, 52(14), 4466-4480.
- [14] Dimitroulis I A. Nintedanib: a novel therapeutic approach for idiopathic pulmonary fibrosis. *Respiratory care*. 2014, 59(9), 1450-1455.
- [15] Richeldi L, Du Bois R M, Raghu G, et al. Efficacy and safety of Nintedanib in idiopathic pulmonary fibrosis. *New England Journal of Medicine*. 2014, 370(22), 2071-2082.
- [16] Roth G J, Binder R, Colbatzky F, et al. Nintedanib: from discovery to the clinic. *Journal of medicinal chemistry*. 2015, 58(3), 1053-1063.
- [17] Egan D, O'kenney R, Moran E, et al. The pharmacology, metabolism, analysis, and applications of coumarin and coumarin-related compounds. *Drug metabolism reviews*. 1990, 22(5), 503-529.
- [18] Noth I, Anstrom K J, Calvert S B, et al. A placebo-controlled randomized trial of warfarin in idiopathic pulmonary fibrosis. *American journal of respiratory and critical care medicine*. 2012, 186(1), 88-95.

- [19] Navaratnam V, Fogarty A W, McKeever T, et al. Presence of a prothrombotic state in people with idiopathic pulmonary fibrosis: a population-based case–control study. *Thorax*. 2014, 69(3), 207-215.
- [20] Roma G, Di Braccio M, Grossi G, et al. Synthesis and in vitro antiplatelet activity of new 4-(1-piperazinyl) coumarin derivatives. Human platelet phosphodiesterase 3 inhibitory properties of the two most effective compounds described and molecular modeling study on their interactions with phosphodiesterase 3A catalytic site. *Journal of medicinal chemistry*. 2007, 50(12), 2886-2895.
- [21] Hongyan Li, Xuguang Zheng, Hongbo Wang, Yi Zhang, Hongqi Xin, Xiaoguang Chen. XLF-III-43, a novel coumarin–aspirin compound, prevents diabetic nephropathy in rats via inhibiting advanced glycation end products. *European Journal of Pharmacology*. 2010, 627, 340-347.
- [22] Bansal Y, Sethi P, Bansal G. Coumarin: a potential nucleus for anti-inflammatory molecules. *Medicinal Chemistry Research*, 2013, 22(7), 3049-3060.
- [23] Manjunath Ghate, R.A. Kusanur, M.V. Kulkarni. Synthesis and in vivo analgesic and anti-inflammatory activity of some bi heterocyclic coumarin derivatives. *European Journal of Medicinal Chemistry*. 2005, 40, 882-887.
- [24] Zhu J, He L, Ma L, et al. Synthesis and biological evaluation of 4-oxoquinoline-3-carboxamides derivatives as potent anti-fibrosis agents. *Bioorganic & medicinal chemistry letters*. 2014, 24(24), 5666-5670.

- [25] Bertelli R, Valenti F, Oleggini R, et al. Cell-specific regulation of alpha1 (III) and alpha2 (V) collagen by TGF- β 1 in tubulointerstitial cell models. *Nephrology, dialysis, transplantation: official publication of the European Dialysis and Transplant Association-European Renal Association*. 1998, 13(3), 573-579.
- [26] Xiao H, Liu R, Ling G, et al. HSP47 regulates ECM accumulation in renal proximal tubular cells induced by TGF- β 1 through ERK1/2 and JNK MAPK pathways. *American Journal of Physiology-Renal Physiology*. 2012, 303(5), F757-F765.
- [27] Thomas A. Wynn, Kevin M. Vannella. Macrophages in Tissue Repair, Regeneration, and Fibrosis. *Immunity*. 2016, 44(3), 452-462.
- [28] Juillerat-Jeanneret L, Aubert J D, Mikulic J, et al. Fibrogenic disorders in human diseases: from inflammation to organ dysfunction. *Journal of medicinal chemistry*. 2018, 61(22), 9811-9840.
- [29] Walraven M, Hinz B. Therapeutic approaches to control tissue repair and fibrosis: Extracellular matrix as a game changer. *Matrix Biology*. 2018, 71: 205-224.
- [30] Fabre A, Marchal-Somme J, Marchand-Adam S, et al. Modulation of bleomycin-induced lung fibrosis by serotonin receptor antagonists in mice. *European Respiratory Journal*. 2008, 32(2), 426-436.
- [31] Moeller A, Ask K, Warburton D, et al. The bleomycin animal model: a useful tool to investigate treatment options for idiopathic pulmonary fibrosis. *The international journal of biochemistry & cell biology*. 2008, 40(3), 362-382.

Highlights

- Hybridization of coumarin skeleton and hydrophobic group of Nintedanib.
- Bioisosteres reduced toxicity of compounds in vitro.
- Inhibition of COL1A1, α -SMA, and p-Smad3 resulted to its attenuation of bleomycin-induced pulmonary fibrosis in mice.

Journal Pre-proof

Declaration of Interest Statement

We declare that we have no financial and personal relationships with other people or organizations that can inappropriately influence our work.

Journal Pre-proof